AD-A159 486 FLOW FIELD EFFECTS ON NUCLEATION IN A REACTING MIXTURE 1/1
LAYER(U) AERONAUTICAL RESEARCH LABS MELBOURNE
(AUSTRALIA) I M KENNEDY NOV 84 ARL-AERO-PROP-R-165

UNCLASSIFIED F/G 7/4 NL

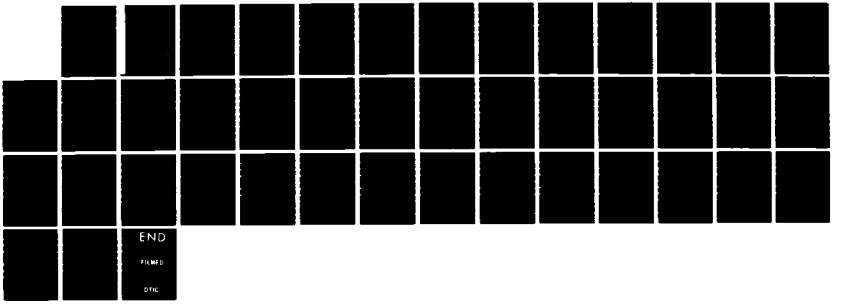

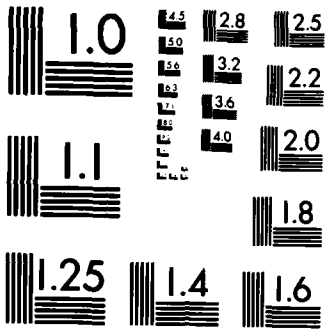

MICROCOPY RESOLUTION TEST CHART
NATIONAL BUREAU OF STANDARDS-1963-A

ARL-AERO-PROP-R-165

AR-003-972

DEPARTMENT OF DEFENCE

DEFENCE SCIENCE AND TECHNOLOGY ORGANISATION

AERONAUTICAL RESEARCH LABORATORIES

MELBOURNE, VICTORIA

AERO PROPULSION REPORT 165

FLOW FIELD EFFECTS ON NUCLEATION IN A REACTING MIXTURE LAYER

by

I. M. Kennedy

COPY No

NOVEMBER 1984

AR-003-972

DEPARTMENT OF DEFENCE
DEFENCE SCIENCE AND TECHNOLOGY ORGANISATION
AERONAUTICAL RESEARCH LABORATORIES

AERO PROPULSION REPORT 165

FLOW FIELD EFFECTS ON NUCLEATION IN A REACTING MIXTURE LAYER

by

I. M. Kennedy

SUMMARY

Chemical nucleation has been studied numerically in a stagnation point mixing layer in which reactants in two counter-flowing streams form a condensable monomer. The response of the subsequent nucleation kinetics to the velocity gradient in the flow is described in terms of a Damkohler number. Two limiting cases have been established. Firstly, if the Damkohler number for monomer production is small, i.e. the rate of monomer production is slow, then the nucleation of particles can be strongly affected by the flow field in a manner which is equivalent to the effect of supersaturation in a uniform vapour. Secondly, if the Damkohler numbers for cluster growth are small (due to a small accommodation factor for monomer-cluster interactions), the concentrations of clusters do not achieve equilibrium levels. This can result in the suppression of particle formation over a critical range of Damkohler numbers. In this case the behaviour of the nucleation kinetics is analogous to the transient phase of nucleation in a uniform vapour.

POSTAL ADDRESS: Director, Aeronautical Research Laboratories,
Box 4331, P.O., Melbourne, Victoria, 3001, Australia

CONTENTS

NOMENCLATURE

a	velocity gradient
C	cluster
$\mathscr{D}$	multicomponent diffusivity
D	Damkohler number
E	internal energy
f	modified stream function
G	Gibbs free energy
$H°$	standardised enthalpy
J	nucleation rate
k	Boltzmann's constant (equations 2–4)
k	rate constant
M	number of cluster size groups
m	molecular weight
n	number of monomers
P	pressure
$\mathscr{R}$	gas constant [m^3 atm $mole^{-1}$ K^{-1}]
R	gas constant
r	radius
$S°$	standardised entropy
S	supersaturation ratio
Sc	Schmidt number
T	temperature
u	tangential velocity
v_L	volume of molecule in liquid phase
v	normal velocity
$\dot{w}$	molar rate of production
x	tangential coordinate
y	normal coordinate
Y	mass fraction
$\dot{y}$	mass flux
ζ	mass accommodation factor
η	non-dimensionalised normal coordinate

μ	dynamic viscosity
ν	kinematic viscosity
ρ	density
σ	surface tension

Superscripts

*	critical cluster
′	differentiation with respect to η
·	differentiation with respect to time
°	at standard conditions

Subscripts

A	reactant *A*
B	reactant *B*
e	at edge of mixing layer
eq	at thermodynamic equilibrium (Section 2.1)
I	inert gas
i	refers to species *i* with *i* monomer units
j	refers to species *j* with *j* monomer units
L	liquid phase
n	number of monomer units
P	product

CAPTIONS TO FIGURES

FIGURE 1 Variation in free energy functions with cluster size.

FIGURE 2 Stagnation point mixing layer flow used in the calculations.

FIGURE 3 Mixing layer velocity profiles.

FIGURE 4 Mass fractions of reactants A and B with distance from cylinder.

FIGURE 5 Estimated Gibbs free energy functions for monomer association.

FIGURE 6 Cluster mass fractions at stagnation point $\zeta = 10^{-4}$ and ΔG_n for NH_4Cl at 400 K.

FIGURE 7 Mass fractions and concentrations at stagnation point of particles containing 200 monomer units

$\zeta = 10^{-4}$ and ΔG_n for NH_4Cl at 400 K.

FIGURE 8 Distribution of clusters through the flow for clusters with

(*a*) 2 monomer units

(*b*) 40 monomer units

(*c*) 80 monomer units

$\zeta = 10^{-4}$ and ΔG_n for NH_4Cl at 400 K.

FIGURE 9 Cluster mass fractions at stagnation point

$\zeta = 10^{-4}$ and ΔG_n for NH_4Cl at 550 K.

FIGURE 10 Cluster mass fractions at stagnation point for slow monomer formation rates

$\zeta = 1$ and ΔG_n for NH_4Cl at 400 K.

FIGURE 11 Mass fractions and concentrations at stagnation point of clusters containing 200 monomer units

$\zeta = 1$ and ΔG_n for NH_4Cl at 400 K.

FIGURE 12 Cluster mass fractions at stagnation point for slow monomer formation rates

$\zeta = 1$ and ΔG_n for MgO at 1700 K.

1. INTRODUCTION

Condensation of a vapour to a liquid in the absence of foreign particles can be described by homogeneous nucleation theory. Experiments usually involve raising the supersaturation of the condensable vapour to a critical level at which observable liquid or solid phase particles are formed. The nucleation rate which is determined by such experiments refers to the formation rate of critically sized clusters of vapour molecules (known as nuclei) which tend to grow as quickly as they evaporate.

In the classical theory the formation of a critical cluster is achieved by the addition of monomer or single vapour molecules to sub-critical clusters. The tendency of a cluster to re-evaporate is determined by a free energy function. Evaluation of this free energy function can be achieved by use of a so-called liquid droplet model in which the properties of a growing cluster are identified with the properties of the bulk liquid phase. Later developments have sought to improve on this estimation of the free energy function. Springer (1978) has reviewed recent advances in homogeneous nucleation theory.

Homogeneous nucleation does not always proceed simply by the supersaturation of pure, condensable vapour. Chemical nucleation designates a process in which the initial formation of a condensable vapour or its subsequent nucleation proceeds by means of chemical reactions. Formation of a condensable vapour by chemical reaction can occur in combustion systems such as rocket exhausts (Courtney, 1962), or in the formation of inorganic oxide aerosols during coal combustion (Katz and Donohue (1982), Neville and Sarofim (1982)). The production of atmospheric aerosols may also be the result of chemical reaction (Friedlander, 1977). The nucleation of soot particles in a flame can be described as a chemical nucleation process in the sense that small molecules add to molecules with increasingly large carbon numbers in a chain of reactions that leads to a macroscopic solid particle. In contrast to physical condensation each step involves chemical bonding: clusters are no longer n-mers formed from a single monomer species but are distinct chemical compounds.

Most practical situations in which chemical nucleation occurs will involve mixing of vapour-phase reactants. Mixing will proceed by diffusive and convective transport.

Diffusive convection in chemically reacting flows has been analysed by Fendell (1965) who considered the effect of the straining motion in a stagnation point flow on ignition and extinction of a diffusion flame. The interaction between diffusion, convection and reaction was analysed in terms of a Damkohler number which was the ratio between a characteristic flow time scale and a characteristic chemical reaction time scale. Extinction of a flame was predicted to occur at a sufficiently low critical Damkohler number, i.e. when the velocity gradient in the stagnation flow was sufficiently high. Values of the critical velocity gradient for counter-flow diffusion flames with various fuels have been measured (Tsuji, 1982). These theoretical and experimental studies were concerned with high activation energy flame reactions which exhibited extinction phenomena in a stagnation point flow. They do suggest, however, a role for the flow yield in influencing the essentially isothermal reactions involved in chemical nucleation in a stagnation point mixing layer.

The involvement of transport processes in nucleation introduces additional phenomena which are not considered in the classical theory for a uniform vapour (for example, Becker and Reiss, 1976). For most simple substances, such as metal vapour which do not involve chemical reactions during their condensation, the time scale for cluster growth and nucleation is considerably shorter than the residence time of the condensing vapour in a flow. This situation applies even in high speed nozzle flows (Wegener and Wu, 1977). However, if the time scale for nucleation processes is increased significantly by chemical reaction so that it is comparable to a characteristic time scale for the mixing flow, the flow may affect the finite rate nucleation kinetics.

The classical theory of nucleation is concerned with a steady-state process. The transient phenomenon which occurs between the achievement of a critical supersaturation and the onset of a steady nucleation rate has been studied numerically in a condensing, uniformly distributed water vapour by Courtney (1962) and Abraham (1969). Analytical treatments of nucleation kinetics by Wakeshima (1954), Collins (1955), Andres and Boudart (1965) and others are essentially in agreement with the numerical predictions for water condensation. The time lag to a steady state is of the order of 1 μ sec; this is considerably shorter than the characteristic time scale for most practical flows. The analysis of the time lag shows, however, a direct proportionality to a mass accommodation or sticking factor which is an indication of the fraction of monomer-cluster collisions that are successful in increasing the cluster size. This factor is believed to be of order unity for substances such as water; for substances which involve chemical reaction in their nucleation it may be much less than one. In the context of nucleation kinetics, an activation energy (E) for the reaction leading to condensable monomer or for the subsequent monomer-cluster reactions may be associated with an accommodation factor, i.e. the term $e^{-E\,RT}$ in an Arrehnius rate expression is equivalent to the accommodation or sticking factor commonly applied in physical condensation processes.

The present study was prompted by the observation of soot or carbon particle formation in a gaseous diffusion flame. The presence of the soot aerosol accounts for the yellow luminosity observed in a sooty flame. Tsuji and Yamaoka (1968, 1970) have reported gas sampling measurements in laminar counter-flow diffusion flames that were stabilized in the forward stagnation point of a porous cylinder. Fuel was blown from the cylinder into a stream of air. They reported a critical velocity gradient (approach flow velocity divided by burner radius) above which no soot was observed to form in the flame, regardless of the rate at which fuel was blown from the burner. For propane and air this critical velocity gradient was about 100 s^{-1}.

Disappearance of the soot occurs at a velocity gradient which is substantially less that the velocity gradient associated with extinction of the flame itself (Tsuji, 1982). Flame temperature is quite insensitive to the approach flow over the velocity range in which soot disappears and, consequently, it is unlikely that the effect has a chemical origin. The sensitivity of the soot formation mechanism to the approach flow velocity is quite marked in this flame. A velocity gradient somewhat less than the critical condition yields a large number concentration of particles in the flame, typically of the order of 10^{16} to 10^{17} m^{-3} (Vandsburger, Kennedy and Glassman, (1984)). An increase in the velocity gradient through increasing the approach flow velocity by as little as 50% can reduce the particle number concentration to zero.

The formation or nucleation of the initial, solid soot particles involves a complex chemical process which is the subject of continuing debate (Glassman, Brezinsky, Gomez and Takahaski (1984), Calcote (1981), Lahaye and Prado (1974)). Regardless of the details of the particular mechanism it is apparent that the formation of a soot particle involves the addition of small molecules to growing larger molecules in a series of reactions leading up to a macroscopic particle. The addition of each small molecule involves chemical bonding often with an associated activation energy which results in a slow growth rate compared with the collision rate. It is one of the aims of this study to explore the possible interaction between the flow field and the kinetics of a nucleation process involving relatively slow chemical reactions.

In order to utilize the observations of soot production in a stagnation point flame and previous analyses of reacting stagnation point flows, the configuration of a laminar counter-flow mixing layer has been adopted for the present numerical study. Specifically, the flow under investigation is in the vicinity of the forward stagnation point of a porous cylinder from which a gaseous reactant is ejected. The other reactant is in the flow which approaches the cylinder.

The balance of reaction and convective-diffusive transport in this flow is affected by the rate of strain, i.e. the velocity gradient. The phenomenon of flame stretch has been shown to result in the extinction of reaction in a stagnation point diffusion flame (Fendell, 1965, Linan, 1974). In the present study the effect of the strain rate or velocity gradient on nucleation kinetics is investigated for two generalized isothermal cases, one in which the formation of condensable monomer is rate limiting, the other for which the subsequent growth reactions are rate limiting. It will be shown for both cases that when the time scale for the rate limiting process is comparable to the time scale for mixing by convection and diffusion, the fluid mechanics can have a significant effect on the nucleation process.

2. HOMOGENEOUS NUCLEATION

2.1 Steady State Theories

A saturated vapour does not condense to the liquid phase in the absence of foreign nuclei until a critical supersaturation is reached. At this condition the onset of nucleation occurs and the supersaturated vapour quickly condenses into liquid. Condensation of the supersaturated vapour occurs by the formation of clusters of monomer units which are drawn together by intermolecular attractive forces. The build-up of these clusters can be represented by a process in which

$$C_1 + C_{j-1} \rightarrow C_j \qquad (j = 2, \ldots\ldots\ldots, M) \tag{1}$$

The increase in size of a cluster C_{j-1} is due to the incorporation of a single monomer. Collisions of clusters with other clusters are assumed to be relatively unimportant in classical theories because of the predominance of monomer in the mixture. Recent theoretical evidence suggests that this assumption might not always be justified (Gelbard and Seinfeld, 1979) for low supersaturations. Clusters can also be reduced in size by the evaporation of monomer in the reverse process.

In order to describe the concentration of clusters of various sizes in a system the classical theory resorts to identification of cluster properties with those of the condensed bulk phase. This is the so-called capillarity assumption. Clusters are treated as small liquid droplets with a bulk free energy and a surface free energy. Formation of a cluster from the vapour phase monomer involves a decrease in bulk free energy for the association of the monomer but an increase in the surface free energy. The change in the Gibbs free energy can be written in terms of liquid phase properties

$$\Delta G_n = -\tfrac{4}{3}\pi r_n^3 \left(\frac{kT}{v_L}\right) \ln S + 4\pi r_n^2 \sigma \tag{2}$$

in which S is the supersaturation ratio (P/P_{eq}) and σ is the surface tension for a flat liquid surface. If ΔG_n is plotted as a function of the number of monomer units in a cluster for a supersaturated vapour then a maximum is evident at n^* (figure 1). For this cluster the increase in ΔG_n due to surface free energy is counterbalanced by the decrease in bulk free energy due to association of n^* monomers. A cluster with n^* monomer units is in a metastable equilibrium with the vapour; evaporation occurs at the same rate as accretion of monomer. This cluster is referred to as the critical size cluster or nucleus and the rate of formation of clusters of the critical size represents the nucleation rate. Once this thermodynamic barrier is surmounted then very rapid growth of a cluster is possible with the subsequent formation of macroscopic condensate particles.

As an example of the classical theory, Frenkel's steady state rate for nucleation is expressed in terms of bulk-phase properties (Frenkel, 1955),

$$J = \left(\zeta \frac{4\pi r^{*2} P}{(2\pi m\, kT)^{1/2}}\right)\left(\frac{\sigma^{1/2} v_L}{2\pi r^{*2} (kT)^{1/2}}\right)\left(\frac{P}{kT} \exp\left(\frac{4\pi r^{*2}\sigma}{3kT}\right)\right) \tag{3}$$

In this equation ζ is a mass accommodation or sticking factor and represents the fraction of collisions which are successful in adding a monomer to a growing cluster. The first term in brackets represents the rate of accretion of monomer. The second term in brackets represents the Zeldovich non-equilibrium factor which accounts for the difference between a metastable equilibrium size distribution of sub-critical clusters and the size distribution attained under steady state conditions. The sensitivity of the nucleation rate to supersaturation arises through the dependence of the critical cluster radius (r^*) on supersaturation (S).

$$r^* = 2\sigma v_L / kT \ln S. \tag{4}$$

Modern theories of nucleation have extended the classical theory by including additional terms in the expression for the change in Gibbs free energy with cluster formation. Evaluation of rotational and translational terms from statistical mechanics is relatively straightforward

but considerable controversy has been generated over the so-called replacement free energy (Zettlemoyer, 1969).

2.2 Transient Nucleation

In a uniform vapour which is brought to a state of critical supersaturation there is a time delay until the onset of steady state nucleation. For most simple substances the estimated time lag is of the order of 1 μ sec which is insignificant in terms of time scales for many practical situations. When chemical reactions are involved in nucleation, however, the time lag may be lengthened so that transient effects are significant throughout a substantial part of a system as suggested by Courtney (1963) for a reacting, condensing rocket exhaust.

Numerical calculations (Courtney (1962), Abraham (1969), Bauer and Frurip (1977)) of the approach to steady state involve integration of a master equation for the population of clusters in the system. The transition probabilities can be based on a droplet model with the use of bulk-phase properties as in equation (2). Alternatively, a Gibbs function defined by extensive thermodynamic quantities can be used to relate forward to backward transition rates, requiring the evaluation of the change in standard enthalpy (ΔH_n°) and entropy (ΔS_n°) for the association of n monomer units into a cluster. This is the approach developed by Frurip and Bauer (1977). It involves the use of a semi-empirical formulation of the enthalpy and entropy changes but avoids the use of the capillarity assumption which is highly dubious for small clusters.

Freund and Bauer (1977) examined theoretical and experimental results for the energy of condensation of an atom onto a cluster. All the substances were metals with the exception of argon. They found that the data could be fitted reasonably well by the expression

$$\Delta E/n = \Delta E_v\,(1-n^{-0.25}) \tag{5}$$

in which $\Delta E/n$ is the energy of condensation per atom for n vapour atoms, ΔE_v is the energy of vapourization or sublimation of the bulk phase, and n is the number of atoms in the cluster. The binding energy per atom in a cluster is less than in the bulk condensed phase as reflected in the lower average density of a cluster. In order to calculate the Gibbs function the enthalpy change for the association of n atoms or molecules is assumed to be approximately equal to the energy change, i.e.

$$\Delta H_n \sim \Delta E_n.$$

Under the conditions of interest this approximation will introduce errors of the order of 10–20% in ΔH_n.

Calculation of the Gibbs function for the association of n monomers is completed by the estimation of the entropy change involved in this process. Bauer and Frurip (1977) analysed the entropy change in terms of changes in a structural entropy component (incorporating translational, rotational and vibrational contributions) and a configurational term which accounts for the number of iso-energetic arrangements that can be adopted by a cluster of monomers. Consideration of experimental data for polymerization reactions and the limiting entropy change for bulk condensation lead Bauer and Frurip to an empirical expression for the structural entropy decrease in the association of n monomers, viz.:

$$\Delta S_n/n = -29n^2/(3+n^2) \tag{6}$$

The configurational term is estimated by counting the number of isomers which are possible for small clusters together with a matching algebraic expression for larger clusters.

The standard Gibbs free energy change for the association of n vapour phase monomers into a cluster, viz.: $nA \rightarrow A_n$ is

$$\Delta G_n^\circ = \Delta H_n^\circ - T\Delta S_n^\circ. \tag{7}$$

For the addition of monomer to a cluster of size n, the free energy increment for the process

$$C_1 + C_n \underset{k_{-n}}{\overset{k_n}{\rightleftharpoons}} C_{n+1}$$

yields the connection between the forward and backward rate constants

$$\frac{k_n}{k_{-n}} = \mathscr{R}T\exp\frac{-(\Delta G_{n+1} - \Delta G_n)}{RT} \tag{8}$$

in which $\mathscr{R}$ has units of [m^3 atm mole^{-1} K^{-1}]. With the ratio between k_n and k_{-n} fixed by equation (8) it is then possible to integrate the master equation for the population of different size clusters in the system.

Bauer and Frurip (1977) studied the Fe vapour system at 1600 K. They found that steady-state conditions were reached in the order of 10^{-7} secs. Their approach yielded a criterion for a cluster of critical size in kinetic terms as one for which the number fluxes of clusters into and out of that size group were approximately equal. The presence of a kinetically determined critical cluster was found not to require a maximum in the Gibbs function as it does in the classical theory.

The kinetic approach does not rely on the use of an equilibrium size distribution with a steady state correction as in the classical analysis. Unfortunately the method is purely computational and fails to provide an analytical solution to the problem. At present, however, it seems that a numerical approach is necessary if one is to consider the entire history of a condensing vapour with the inclusion of the initial transient phase.

2.3 Chemical Nucleation

Nucleation of condensable vapours in a number of reacting flows can exhibit transient-like effects. Courtney (1963) concluded that the condensation of some non-volatile reaction products in rocket exhausts fueled by lithium and boron propellants could be described, in some circumstances, as a non-steady state nucleation process because the time lag was comparable to the residence time in a nozzle. The room temperature nucleation of NH_4Cl particles from reacting HCl and NH_3 vapours has been studied by Henry, Gonzalez and Peters (1983) in a flow reactor. They reported induction times of the order of 2 seconds between the initial rapid mixing of the two reactants and the onset of nucleation. This period of the flow is certainly non-steady. These two examples illustrate situations in which the production of condensable monomer is slow relative to time scales of a flow. The production of soot in a flame is a case in which the nucleation process itself is relatively slow. The effects of mixing and fluid flow on nucleation in these systems has been given little attention in the past.

A generalised model has been set up to investigate nucleation phenomena in a counter-flow stagnation point configuration. A condensable monomer is assumed to be produced by the irreversible one-step reaction between reactants *A* and *B* which are diluted to initial mass fractions of 0·1% in an inert carrier gas. Reactant *A* is in the gas stream issuing from a porous cylinder and reactant *B* is in the free-stream flow as shown in figure 2. The reaction between the two species is assumed to follow the stoichiometry described in equation (9)

$$A + B \rightarrow P \tag{9}$$

in which the combination of 1 mole of *A* and 1 mole of *B* combine to yield 1 mole of product *P*. This stoichiometry locates the zone of maximum formation rate of product at the stagnation point of the flow. It will be seen later that this choice of stoichiometry facilitates interpretation of the results without a concomitant reduction in generality.

As product is formed it is allowed to simultaneously nucleate by the formation of clusters via reversible reactions of the form

$$C_1 + C_1 \rightleftharpoons C_2$$

$$C_1 + C_{n-1} \rightleftharpoons C_n \qquad n = 3, \ldots, M.$$

Two limiting cases have been studied. They correspond to firstly the situation in which production of condensable monomer is slow compared with the subsequent nucleation steps and, secondly, to the case when the nucleation steps are slow compared with monomer production rates because of small accommodation factors. The latter situation can arise when cluster growth involves chemical reaction with an activation energy which can be associated with a non-unity accommodation factor.

Both cases have been studied for isothermal conditions. Rates of monomer production for the first case have been chosen to correspond approximately to the reaction of NH_3 and HCl at 400 K with a rate constant of approximately 10 to 100 m^3/s-mole (Countess and Heicklen, 1973). The standard Gibbs free energy function has been determined from the heat of sublimation of NH_4Cl (39·9 kcal/mole) by the approach of Bauer and Frurip (1977) discussed in Section 2.2. Monomer-cluster collision rates are based on hard sphere rates from kinetic theory and the accommodation factor for monomer-cluster collisions is unity. Use of these numerical values is only a convenient means for ascribing the rate constants and Gibbs free energy functions in this purely numerical study; the use of different Gibbs functions demonstrates the generality of the analysis. The rate constants occur only in combination with the flow velocity gradient (as a Damkohler number in Section 4) and their absolute values are not of immediate concern in this study. Accurate values of the rate constants would be necessary if an attempt were made to deduce velocity gradients from a Damkohler number for a specific case.

In the second case monomer production and monomer-cluster collisions are again taken to occur at hard sphere collision rates derived from kinetic theory. However, in this case the growth rate of clusters is slow compared with the production rate of condensable monomer due to a small accommodation factor. This factor accounts for the fraction of monomer-cluster collisions which are successful in leading to incorporation of the monomer into the cluster. For many simple substances it is of order unity. The situation of present interest, however, describes a nucleation process in which the accommodation factor is much less than one due to the involvement of chemical reactions in the bonding of monomer to cluster. The accommodation factor in the calculations has been chosen as 10^{-4}. At 400 K this value corresponds to an activation energy for monomer bonding of 7·4 kcal/mole and at 2000 K to an activation energy of 36 kcal/mole. The latter value is representative of reaction activation energies in a diffusion flame.

3. STAGNATION POINT FLOW

Figure 2 illustrates the flow configuration that has been studied. Gas which is seeded with reactant A is ejected uniformly around the circumference of a porous cylinder. The cylinder is situated in an approaching flow which is seeded with reactant B and which is of uniform velocity far upstream of the cylinder. The region of interest is in the vicinity of the forward stagnation point where a local similarity solution for the flow field is valid. The advantage of analysing this stagnation point flow is that a similarity solution permits the reduction of the partial differential equations for mass, momentum and energy to ordinary differential equations with one independent variable.

The boundary layer form of the momentum equation in the x-direction is given by

$$\rho u \frac{\partial u}{\partial x} + \rho v \frac{\partial u}{\partial y} = \frac{\partial}{\partial y}\left(\mu \frac{\partial u}{\partial y}\right) - \frac{dP}{dx} \tag{10}$$

In the inviscid flow outside the boundary layer the pressure gradient is

$$-\frac{dP}{dx} = \rho u \frac{du_e}{dx} \tag{11}$$

$$= \rho u a$$

where a is the imposed velocity gradient.

A transformed normal coordinate is introduced

$$\eta = \left(\frac{a}{\nu}\right)^{1/2} y. \tag{12}$$

The equation of continuity is satisfied by relating both velocity components to a modified stream function, f, so that

$$u = u_e f' \tag{13}$$

where the prime denotes a derivative with respect to η and

$$v = (a\nu)^{1/2} f \tag{14}$$

After some manipulation the transformed momentum equation becomes

$$f''' + ff'' - f'^2 + 1 = 0. \tag{15}$$

The boundary layer for the conservation of mass fraction, Y_i, of species, i, is

$$\rho u \frac{\partial Y_i}{\partial x} + \rho v \frac{\partial Y_i}{\partial y} = \frac{\partial}{\partial y}\left(\rho \mathscr{D}_i \frac{\partial Y_i}{\partial y}\right) - m_i \dot{w}_i. \tag{16}$$

In this equation $\mathscr{D}_i$ is a binary diffusivity of species i in the mixture. The reaction rate term, $\dot{w}_i$, is the net molar rate of production of species i where m_i is the molecular weight of this species and the stoichiometric coefficient for the reaction of equation (9) is unity.

When the similarity transformation is applied to this equation the result is

$$\frac{1}{Sc_i} Y_i'' + f Y_i' = \frac{m_i \dot{w}_i}{a\rho} \tag{17}$$

where Sc_i (Schmidt number) for species i is defined as

$$Sc_i = \frac{\nu}{\mathscr{D}_i}. \tag{18}$$

For an irreversible one-step reaction such as

$$A + B \rightarrow P \tag{19}$$

the rate of production of product P is expressed as

$$\dot{w}_P = k_P [A] [B] \tag{20}$$

In terms of mass fractions equation (20) reads as

$$\dot{w}_P = k_P \frac{\rho Y_A \rho Y_B}{m_A \; m_B}. \tag{21}$$

The conservation equation for the mass fraction of product P is

$$\frac{1}{Sc_P} Y_P'' + f Y_P' = -\begin{pmatrix} m_P & \rho k \\ m_A \; m_B & a \end{pmatrix} \cdot Y_A \; Y_B. \tag{22}$$

The first group of terms on the right hand size defines a Damkohler number

$$D_P = \frac{m_P \quad \rho k}{m_A \; m_B \; a} \tag{23}$$

which expresses a ratio between a characteristic flow time (through a^{-1}) and a characteristic chemical reaction time $\left(\text{through } \begin{matrix} m_A \; m_B & 1 \\ m_P & \rho k \end{matrix}\right)$. Boundary conditions at the cylinder surface and in the free stream are required to complete the specification of the problem.

At the cylinder wall the ejection velocity of gas is v_W. The stream-function at the wall ($\eta = 0$) is then given by

$$f(0) = -v_W / \sqrt{a\nu}. \tag{24}$$

Reactant A is ejected from the cylinder and reactant B is in the free-stream flow (see figure 2). A convective-diffusive balance at the wall gives the following boundary conditions for the mass fractions of A and B

$$Y_A(0) = Y_I - Y_A'(0)/Sc_A \cdot f(0) \tag{25}$$

and

$$Y_B(0) = - Y_B'(0)/Sc_B \cdot f(0), \tag{26}$$

Y_I is the mass fraction of inert carrier gas.

In the free-stream

$$f' = 1,$$

$$Y_A = 0,$$

and

$$Y_B = 1 - Y_1. \tag{27}$$

Nucleation is treated by solving a set of simultaneous equations of the form of equation (22) for the mass fractions of clusters. The Schmidt number of a cluster is derived from the kinetic theory for diffusivities (Hirschfelder, Curtiss and Bird (1954)). The rate constant for a collision between a cluster with i monomer units and a single monomer is assumed to increase with $i^{2/3}$ as spherical cluster sizes increase.

Solution of the problem entails the definition of the flow field through equation (15) for a given ejection velocity and approach velocity followed by solution of the coupled equations for Y_A and Y_B. This step is followed by the simultaneous solution of coupled equations for the production of monomer and larger clusters with kinetics (discussed in Section 2.3) that are characterised by a Damkohler number for monomer production (D_1) and Damkohler numbers (D_i, $i = 2 \ldots .., M$) based on the rate constant and molecular weight for the growth of a cluster with i monomer units. The results are reported for conditions specified by D_1 and D_2 where D_2 is the Damkohler number for monomer–monomer collisions.

4. SOLUTION PROCEDURE

The equation for momentum (15) and the equations for species mass fractions (22) are written in central difference forms. The solutions of the resulting tri-diagonal systems of equations are obtained implicitly with a Gauss elimination procedure for 120 equally spaced grid-points with an interval in η of 0·04. Iteration of the calculations is continued until the relative difference between successive iterations at a grid point is less than 0·001. The non-linearities in the momentum equation and the equation for monomer mass fraction (the term involving $Y_1 \times Y_1$) are handled by quasi-linearization (Bellman and Kalaba, 1965). Refinement of the grid spacing by 25% to intervals in η of 0·03 results in differences in computed cluster concentrations of less than 1%.

The non-dimensional blowing rate from the cylinder is $f(0) = -1{\cdot}0$ for all cases. The stoichiometry of reaction (equation (9)) between reactants in the flow from the cylinder and in the free-stream is chosen so that the stoichiometric coefficients of A and B in (9) are 1, i.e. one mole of A reacts completely with 1 mole of B. Both reactants are diluted in an inert carrier gas so that their mass fractions in the feed-streams are 0·001 and the mass fraction of inert gas is constant throughout the flow.

Damkohler numbers are based on a gas density of 1·18 kg m^{-3}, stoichiometric coefficients of 1, and a molecular weight of condensable monomer (NH_4Cl) of 53 kg kmole^{-1}. A Damkohler number of 10^8 with a bimolecular collision rate constant of 10^8 m^3 mole^{-1} sec^{-1} corresponds to a velocity gradient of 23·7 sec^{-1}. If the cylinder radius were 10 mm then the approach flow velocity which is required far upstream to achieve this condition would be 118 mm sec^{-1}. It follows that the approach flow velocity which is required to yield a Damkohler number of 10^6 is 11·8 m sec^{-1}.

Damkohler numbers for the production of clusters are modified by increases in the molecular weight of clusters and by increases in the collision rate as cluster size increases. For clusters of particles which incorporate more than 20 monomer units averaged conversion rates are used in the same manner as Jensen (1974), so that if the number of monomers in a cluster is n_i and $n_i < n_j$ then for the process $C_1 + C_i \cdots C_j$

$$\frac{d[C_1]}{dt} \quad \frac{d[C_j]}{dt} \quad \frac{1}{(n_j \quad n_i)} k_j [C_1] [C_i]. \tag{28}$$

The Damkohler number D_j is based on the averaged rate constant $k_j/(n_j \quad n_i)$.

A limit must be set in the calculations on the maximum allowable size of cluster or particle. The present calculations involve removal of particles greater than this size from the system. Because cluster–cluster interactions are not considered, the primary effect of changing the upper

size limit is to change the rate of loss of monomer via particle growth. All the results which are presented are obtained by considering particles containing up to 240 monomer units.[1] Some cases have been computed with a maximum allowed particle size of 10 monomer units; the effect of cluster concentrations compared with the full calculation is less than 0·01%. This is due to very low concentration of clusters which contain more than a few monomer units; extension of the computations to clusters of 240 units serves essentially to give a clearer representation of the behaviour of the system. However, termination of the calculations at 240 monomers ignores the role of larger aerosol particles which can contribute to significant heterogeneous nucleation. This question is addressed in a later section.

5. EFFECT OF MIXING ON NUCLEATION

5.1 Reacting Stagnation Point Flow Field

The reactions which are included in the model are not significantly endothermic or exothermic at low concentrations. Consequently, there is no effect of chemical reaction or condensation on the flow field. The flow is the same for all the cases which have been modelled and can be solved independently of the nucleation kinetics. At the cylinder wall the non-dimensional blowing velocity $f(0)$ is $-1\cdot0$. The two velocity components, viz.: $v = -f(av)^{1/2}$ and the tangential component u/u_e where u_e is the velocity at the boundary layer edge, are shown in figure 3 as functions of the non-dimensional normal coordinate, η where

$$\eta = \left(\frac{a}{\nu}\right)^{1\cdot2} y.$$

The tangential velocity, u, exhibits a laminar boundary layer profile. The thickness of the layer scales with $(\nu/a)^{1/2}$. The normal velocity component indicates that the stagnation point is at about $\eta = 1\cdot9$. The distance of the stagnation point from the cylinder will vary with $(\nu/a)^{1/2}$ for a fixed gas ejection velocity. Calculations of nucleation kinetics are performed with these flow conditions.

The interaction between the flow field and nucleation is determined by the Damkohler number as discussed in Section 4. If the Damkohler number is small then chemical reaction is slow compared to residence time in the flow. The effect of Damkohler number on the reaction of two species contained in the two mixing streams is shown in figure 4. For the reaction rates, densities etc., chosen in Section 5, a Damkohler number of 10^8 corresponds to a velocity gradient of $23\cdot7\ \text{sec}^{-1}$. With one mole of reactant A consuming one mole of reactant B the reaction zone is located in the vicinity of the stagnation point. For low velocity gradients ($D_1 = 10^8$) the region of reaction is narrow with little overlap of reactants. As the velocity gradient is increased ($D_1 = 10^6$) there is considerably more interpenetration of reactants.

5.2 Free Energy Functions

Standard Gibbs free energy functions for use in the computation of nucleation kinetics have been determined using the empirical approach of Bauer and Frurip (1977). Enthalpies and entropies are estimated from curves fitted to theoretical and experimental data (see Section 2.2). The substances considered by Bauer and Frurip were monatomic species; the use of their empirical correlations for polyatomic species involves some uncertainty. However, it will be shown that the choice of the Gibbs function does not significantly alter the overall behaviour of the nucleation kinetics. The system that has been modelled in most cases consists of NH_4Cl vapour for which the estimated Gibbs functions at 400 K and 550 K are shown in figure 5 in a dimensionless form.

At 400 K the Gibbs function very quickly attains large negative values which indicate stable clusters. There is no maximum in the curve. At 550 K (61 K below the temperature of sublimation) the Gibbs function exhibits a maximum at a cluster with 3 molecules and does

[1] Based on the bulk density of NH_4Cl the diameter of these particles is about 3 nm.

not attain negative values until clusters contain more than 6 molecules. Also shown in figure 5 is the Gibbs function for MgO at 1700 K. Neville and Sarofim (1982) reported a study of particle production from inorganic vapours evolved during the combustion of coal. Magnesium oxide particles were formed by the nucleation of the oxide vapour which was, in turn, produced by the oxidation of magnesium vapour around a coal particle. The magnesium oxide system affords an additional case to which a kinetic scheme can be applied and permits an evaluation of the generality of the conclusions which have been reached. It can be seen from figure 5 that MgO vapour condenses quite readily at 1700 K with the Gibbs function rapidly attaining negative values. Clusters with more than 4 or 5 molecules are quite stable according to these estimates of the free energy.

5.3 Nucleation

5.3.1 Fast Vapour Formation: Slow Nucleation ($D_1 \gg 1$, $\zeta = 10^{-4}$)

If the formation of a cluster involves chemical bonding then the accommodation or sticking factor for monomer-cluster interactions will be less than one. The accommodation factor, ζ, is chosen to be 10^{-4} in these calculations (see Section 2.3). Damkohler numbers for cluster formation are then related to D_1 as $D_j = \{j^{5/3}/(j-1)\}\zeta D_1$, $j = 2, \ldots, M$ where the terms in j account for variations in molecular weights and collision rates with cluster size.

In the absence of a simple, chemically reacting system to which this model can be applied, the Gibbs function for NH_4Cl vapour at 400 K has been used in the calculations. This choice aids in the comparison of the results with those obtained in the following section.

Three velocity gradient conditions have been used to yield D_1 of 10^8, 10^7 and 10^6. Calculated mass fractions for various size clusters or particles are shown in figure 6 at these three values of Damkohler number. It is apparent from figure 6 that the nucleation process is very sensitive to flow conditions when cluster growth is slow. For $D_1 = 10^8$, the mass fraction of clusters with 80 molecules is 2×10^{-8} which corresponds to about 3×10^{15} clusters m^{-3}. When the approach flow velocity is increased by a factor of 10 so that $D_1 = 10^7$, the mass fraction of clusters with 80 molecules reduces by three orders of magnitude to about 2×10^{-11} or 3×10^{12} clusters m^{-3}. With a further increase in the approach flow velocity by an order of magnitude so that $D_1 = 10^6$, the concentrations of clusters of any significant size are negligible. The production of larger particles has been suppressed, in effect, by controlling the flow field.

The sensitive response of particle formation to changes in the velocity gradient is illustrated more directly in figure 7 for a range of Damkohler numbers. The mass fractions and number concentrations of particles with 200 monomer units at the stagnation point of the flow are shown as functions of a Damkohler number. For large Damkohler numbers there is a relatively weak dependence of particle concentration on velocity gradient. However, at a Damkohler number of around $5{\cdot}0\times10^7$ kinetic effects start to become dominant and the concentration of particles begins to decrease rapidly. At a Damkohler number of about 2×10^6 there are effectively no large particles in the flow.

It was pointed out in Section 5 that these calculations involve the removal of particles with more than 240 monomer units from the system. In fact, with a large Damkohler number there will be a substantial amount of larger aerosol particles present in the flow as the results presented in figure 6 suggest. For D_1 of 10^8 there is little diminution of mass fractions of clusters with up to 240 monomer units.

Friedlander (1982) demonstrated in a numerical calculation that an aerosol can scavenge monomers and clusters and can reduce the nucleation rate significantly. Condensation onto an existing particle provides an alternative route in contrast to homogeneous nucleation for gas to particle conversion. The present calculations have been limited to 240 monomer units by the restriction of available computing services and by the numerical difficulty of incorporating large particles into the study. The latter difficulty arises as the diffusivities of large particles become quite small and the Schmidt numbers become correspondingly large. The inverse Schmidt number multiplies the highest order term in equation (17). As the Schmidt number becomes large the problem tends to become singular as the governing equation is reduced from

second to first order. The numerical difficulties which arise from considering large aerosol particles in the mixing layer have precluded their consideration in this study.

The behaviour of the nucleating mixing layer will be unaffected by an aerosol at high velocity gradients (small Damkohler numbers) for which the mass fractions or large clusters are negligible. For low velocity gradients the nucleation rate will be reduced and the cluster size distribution will be modified by the presence of an aerosol. However, it is expected that the qualitative behaviour of the system will be similar.

A comparison of the results presented in figure 6 with those of Bauer and Frurip (1977) for a kinetic nucleation model of iron vapour condensation reveals similarities between the two sets of calculations. The sensitive response of nucleation kinetics in the stagnation point flow to changes in the velocity field is analogous to the transient conditions computed by Bauer and Frurip for their nucleating, uniform, iron vapour system. The population of large clusters was very small in their calculations for periods of 10^{-10} to 10^{-9} secs after the initiation of cluster growth at a supersaturation ratio, S, of 3040. By 10^{-7} secs their system had reached a steady-state with significant levels of large clusters. The behaviour of the nucleating stagnation point flow appears to be directly analogous to this transient nucleation phenomenon.

The distribution of clusters of different sizes throughout the flow is shown in figure 8 for a Damkohler number of 10^8. The peaks in cluster concentration occur at the same location close to the stagnation point of the flow. At this point the effects of diffusion and convection of clusters are small because of the near zero concentration gradients and velocity. As a result it is possible to estimate the mass flux from one size group to another without a significant complication due to transport processes.

Using a value of the rate constant for monomer–monomer interactions of 10^8 m^3 mole^{-1} sec^{-1} and $\zeta = 10^{-4}$ it is possible to derive the mass flux in cluster size space ($\dot{\gamma}$) in one direction for a given size cluster, i.e. $\dot{\gamma}_{i\to i+1}$ is the mass flux (kg m^{-3} s^{-1}) for conversion of clusters with i monomers to $i+1$ monomers while $\dot{\gamma}_{i\leftarrow i+1}$ is the mass flux in the reverse direction. Table 1 presents these mass fluxes for two cases, viz.: $D_1 = 10^8$ and $D_1 = 10^6$.

When $D_1 = 10^8$, i.e. when the approach flow velocity is low, the forward and backward fluxes are balanced for small clusters. At the cluster size associated with the 'knee' in the mass fraction curve of figure 6, the forward and backward fluxes are nearly balanced, and, in addition, the two forward fluxes into and out of this size group are approximately equal (within an order of magnitude). For the $D_1 = 10^8$ case the 'knee' is at about $n = 3$ so that $\dot{\gamma}_{2\to3} \sim \dot{\gamma}_{2\leftarrow3} \sim \dot{\gamma}_{3\to4} \sim \dot{\gamma}_{3\leftarrow4}$. Bauer and Frurip (1977) identified this condition as the specification of a kinetically determined critical cluster size. The critical cluster marks the point of a switch-over in the kinetics; the population of small clusters is established by balanced forward and backward conversion rates while the population of larger clusters is maintained by nearly equal forward conversion rates with negligible backward rates (for example $\dot{\gamma}_{17\to18} \sim \dot{\gamma}_{18\to19}$ and $\dot{\gamma}_{17\leftarrow18} \sim \dot{\gamma}_{18\leftarrow19} \sim 0$). As noted by Bauer and Frurip (1977) the presence of a critical cluster in the kinetics calculation does not require a maximum in the Gibbs function as it does in the classical theory. The computed behaviour of the system modelled with NH_4Cl vapour at 400 K for which there is no maximum (figure 5) is essentially the same as at 550 K (figure 9) for which a maximum in the Gibbs function is evident.

For a higher approach flow velocity ($D_1 = 10^6$) Table 1 indicates that the forward and reverse fluxes for clusters with more than one monomer unit are never equal, i.e. the reversible processes involved in cluster growth are not equilibrated even for small clusters. At larger sizes the predominant flux is the forward one but it continues to decrease with increasing cluster size. From these results it is evident that small cluster concentrations do not have a chance to equilibrate within the time scale imposed by the velocity gradient. As a result larger clusters cannot establish significant concentrations. This behaviour is directly analogous to a transient nucleation phenomenon.

In order to demonstrate that the form of the results are not specific to a particular choice of the free energy function, the calculations for $D_1 = 10^8$ and $D_1 = 10^6$ have been repeated with an estimated free energy function for NH_4Cl at 550 K. The mass fractions for various size clusters are shown in figure 9. The bend or knee in the curves is shifted to larger clusters ($n \sim 9$) and the concentrations are substantially lower. If the cluster for which the four fluxes ($\dot{\gamma}_{i-1\to i}$, $\dot{\gamma}_{i-1\leftarrow i}$, $\dot{\gamma}_{i\to i+1}$, $\dot{\gamma}_{i\leftarrow i+1}$) are approximately equal (i.e. at the 'knee' in the mass fraction curve)

is taken to be a critical size cluster or nucleus then the nucleation rate for $D_1 = 10^8$ at 400 K is of the order of 10^{20} m^{-3} s^{-1}. At 550 K the nucleation rate is of the order of 10^7 m^{-3} s^{-1}.

Despite the different concentrations of large clusters, the response of the nucleation process to changes in Damkohler number is much the same at 400 K and 550 K. At $D_1 = 10^8$ there is only a very gradual decay in the number concentration of large particles with size while at $D_1 = 10^6$ there are effectively no large particles. The critical range of Damkohler numbers which determines the cessation of nucleation evidently does not depend strongly on the free energy function. It must be noted, however, that at higher temperatures the rate constants for cluster growth will be larger and, consequently, the velocity and velocity gradient must be correspondingly larger to achieve a certain Damkohler number. Whenever the nucleation Damkohler numbers, D_i, $i = 2, \ldots, M$, are sufficiently small due to a small accommodation factor the flow field effect reported here is possible.

Although the model which has been developed here for nucleation in a stagnation point flow is isothermal and represents a limiting case for which condensable monomer production is fast, it affords some insight into the response of a sooting diffusion flame to variations in the local flow field. The formation of soot occurs at high temperatures around 1800 K on the fuel side of a flame. There is no identifiable single species, i.e. monomer which leads directly to soot particles via polymerization reactions although the polyacetylene mechanism of Homann and Wagner (1967) relies upon such a route up to the point of aromatic ring formation. The formation of polycyclic aromatic compounds (building blocks for soot particles) from straight chain aliphatic fuels poses a mechanistic problem for kinetic schemes of soot formation (Cole, Bittner, Longwell and Howard, 1984). However, once aromatic compounds such as benzene or toluene have been formed in the flame, growth of more stable, larger polyaromatic species can proceed by the addition of abundant stable species such as acetylene or highly reactive radicals. Stein (1978) has used group additivity methods to analyse the high temperature equilibria of acetylene and polyaromatic species. He suggested a route which is favoured thermodynamically for the formation of a large polycyclic aromatic, $C_{96}H_{21}$. The Gibbs functions for the formation of these polyaromatics are similar in form to the Gibbs functions for NH_4Cl association which are used in the present model.

The formation of condensable monomer is assumed to be much faster than the subsequent nucleation in this model; the formation of acetylene and other pyrolysis products in a flame may not approach this limiting rate. However, data for stagnation point diffusion flames (Tsuji, 1982) indicate constant flame temperatures and presumably, constant pyrolysis rates over the range of velocity gradients in which soot formation is suppressed.

Despite the differences between the model and the complex kinetics of soot formation in a diffusion flame the overall nucleation mechanisms are sufficiently similar to allow some conclusions to be drawn. If the formation of polyaromatic compounds in a flame involves relatively slow kinetics at some stage, a large velocity gradient in a stagnation flow may reduce species concentrations substantially below equilibrium levels. The result of non-equilibrium concentrations of the least stable, small precursor molecules in the nucleation chain would be greatly reduced rates of macroscopic particle formation.

5.3.2 Slow Vapour Formation: Fast Nucleation ($D_1 \sim 1$, $D_i \gg 1$, i 2, . . ., M)

For most condensing vapours the accommodation coefficient $\zeta \sim 1$ so that cluster growth is limited by the collision rate between monomer and clusters. However, when a condensable vapour is the product of a chemical reaction such as in a rocket exhaust (Courtney (1963)), during coal combustion (Katz and Donohue (1982), Neville and Sarofim (1982)) or a simple room temperature reaction such as HCl and NH_3 (Countess and Heicklen (1973), Henry *et al.* (1983)) the rate of monomer formation may be the limiting step in the nucleation of particles. The Damkohler number for monomer formation, D_1, may be of order 1 for practical reaction rates and velocity gradients.

Calculations have been performed for the HCl NH_3 system in a stagnation point mixing layer. The rate constant of Countess and Heicklen (1973) for the HCl NH_3 reaction suggests values of D_1 60, 6 and 0·6 for realistic velocity gradients. The computer simulation has been carried out to model the effect of varying velocity gradients when D_1 is small. As D_1 decreases

from 60 to 0·6, D_2 for monomer–monomer collisions decreases from 10^8 to 10^6. The mass accommodation factor ζ is 1. The Gibbs free energy function for NH_4Cl at 400 K has been used.

The mass fractions of clusters at the stagnation point are shown in figure 10 for three cases with different velocity gradients. Monomer concentrations decrease by two orders of magnitude as the velocity gradient is increased by two orders of magnitude. There is a much more pronounced effect on the concentration of larger clusters. An increase in the velocity gradient by two orders of magnitude results in 13 orders of magnitude decrease in large cluster mass fractions. The size of the kinetically determined 'critical' cluster increases from about 4 molecules at the highest Damkohler number to about 6 at the lowest Damkohler number. Based on the concentration of these clusters the nucleation for $D_1 = 60$ is about 10^{11} m^{-3} s^{-1} and for $D_1 = 0{\cdot}6$ is about 10^{-2} m^{-3} s^{-1}. The latter rate is so low that particle formation is negligible.

The mass fluxes for various processes are shown in Table 2. It can be seen that forward and backward rates are equilibrated for small clusters for both high and low Damkohler numbers. This behaviour is in contrast to the previous case (Section 5.3.1) in which nucleation was slow compared with monomer formation. For those conditions a low Damkohler number (high velocity gradient) prevented equilibration of forward and backward rates for even the smallest clusters. As a result nucleation behaviour was characteristic of a transient phenomenon. In the present case for which monomer production is rate limiting the behaviour is characteristic of a steady state system for all the velocity conditions which have been computed. The response of the nucleation process to velocity gradient changes is typical of the sensitive response of a nucleating, uniform vapour to variations in supersaturation.

The monomer mass fraction when $D_1 = 60$ is 6×10^{-5} and when $D_1 = 0{\cdot}6$ is 7×10^{-7}. Two orders of magnitude variation in supersaturation can give rise to extremely large differences in nucleation rates as the classical theory indicates via equations (3) and (4). Hence the effect of flow conditions on nucleation rates in the mixing layer for this case can be interpreted in terms of the analogy with the very strong effect of supersaturation in a uniform vapour. The influence of flow conditions is shown directly in figure 11 for the mass fractions of particles with 200 monomer units. The curve is consistent with the supersaturation analogy.

In order to check on the generality of these observations for other systems a calculation has been performed with the estimated Gibbs function for MgO vapour at 1700 K. The Gibbs function is shown in figure 5. It corresponds to the conditions studied by Neville and Sarofim (1982) for MgO particle formation during coal combustion. In keeping with the findings of Neville and Sarofim (1982) the condensable MgO vapour is assumed to be formed by the gas-phase oxidation of magnesium vapour. Varying the Damkohler numbers by changing the velocity gradient over two orders of magnitude produces the same effect for the MgO system (see figure 12) as the NH_4Cl system. That is, mass fractions of small clusters are equilibrated; the response to the reduced formation rate of vapour (reflected in two orders of magnitude decrease in monomer concentration) is equivalent to a reduction in supersaturation in a uniform gas.

CONCLUSIONS

Chemical nucleation in a reacting mixing layer has been modelled numerically with an isothermal, stagnation point flow. Reactants in two mixing streams form a condensable monomer product which subsequently undergoes nucleation through the formation of clusters. The relevant time scale for convective–diffusive transport in the stagnation point flow is the inverse rate-of-strain, i.e. the inverse velocity gradient in the vicinity of the stagnation point. Calculations show that when the time scale for the rate limiting chemical reaction in the nucleation process is comparable to the time scale imposed by the flow field, nucleation can be suppressed.

Two limiting cases have been investigated. When the formation rate of condensable monomer is slow, nucleation in the mixing layer exhibits a sensitive response to the velocity gradient. The concentrations of small clusters are equilibrated with monomer concentration for all flow conditions and the effect of the flow field on nucleation is analogous with the effect of the supersaturation ratio in a uniform gas. However, when monomer–cluster reactions are rate limiting because of a small accommodation factor, the sensitive response of the nucleation kinetics to variations in velocity gradient follows a different route. Over a critical range of velocity gradients the concentration of small clusters cannot establish equilibrium levels. The non-equilibrium

concentrations of small clusters results in the suppression of particle formation for high velocity gradients.

The suppression of soot formation in a stagnation point diffusion flame at a critical velocity gradient can be understood in terms of the latter mechanism. The effect on nucleation kinetics of the mixing rate may be significant in other reacting flows such as turbulent diffusion flames and rocket exhausts.

REFERENCES

Abraham, F. F. (1969). Multistate kinetics in nonsteady state nucleation; A numerical solution. J. Chem. Phys. *51*, 1632–1638.

Andres, R. P., and Boudart, M. (1965). Time lag in multistate kinetics: Nucleation. J. Chem. Phys. *42*, 2057–2064.

Bauer, S. H., and Frurip, D. J. (1977). Homogeneous nucleation in metal vapors 5: A self-consistent kinetic model. J. Phys. Chem. *81*, 1015–1024.

Becker, C., and Reiss, H. (1976). Nucleation in a nonuniform vapour. J. Chem. Phys. *65*, 2066–2070.

Bellman, R. E., and Kalaba, R. E. (1965). *Quasilinearization and Nonlinear Boundary Value Problems*, American Elsevier.

Calcote, H. F. (1981). Mechanisms of soot nucleation in flames—A critical review, Combustion and Flame, *42*, 215–242.

Cole, J. A., Bittner, J. D., Longwell, J. P., and Howard, J. B. (1984). Formation mechanisms of aromatic compounds in aliphatic flames. Combustion and Flame, *56*, 51–70.

Collins, F. C. (1955). Time lag in spontaneous nucleation due to non-steady state effects. Z. Elektrochem. *59*, 404–407.

Countess, R. J., and Heicklen, J. (1973). Kinetics of particle growth II Kinetics of the reaction of ammonia and hydrogen chloride and the growth of particulate ammonium chloride. J. Phys. Chem. *77*, 444–447.

Courtney, W. G. (1962). Non-steady state nucleation. J. Chem. Phys. *36*, 2009–2017.

Courtney, W. G. (1963). Condensation in nozzles. *Ninth Symposium (International) on Combustion*, 799–810, Academic Press.

Fendell, F. E. (1965). Ignition and extinction in combustion of initially unmixed reactants. J. Fluid. Mech. *21*, 281–303.

Frenkel, J. (1955). *Kinetic theory of liquids*. Dover.

Freund, H. J., and Bauer, S. H. (1977). Homogeneous nucleation in metal vapours 2: Dependence of the heat of condensation on cluster size. J. Phys. Chem. *81*, 994–1000.

Friedlander, S. K. (1982). The behaviour of constant rate aerosol reactors. Aerosol Sci. and Tech. *1*, 3–13.

Frurip, D. J., and Bauer, S. H. (1977). Homogeneous nucleation in metal vapours 4: Cluster growth rates from light scattering. J. Phys. Chem. *81*, 1007–1015.

Gelbard, F., and Seinfeld, J. H. (1979). The general dynamic equation for aerosols: Theory and application to aerosol formation and growth. J. Colloid Interface Sci. *68*, 363–382.

Glassman, I., Brezinsky, K., Gomez, A., and Takahashi, F. (1984) Physical and Chemical kinetic effects in soot formation, in *Recent Advances in Aerospace Science*, ed. C. Casci, Plenum Press.

Henry, J. F., Gonzalez, A., and Peters, L. K. (1983) Dynamics of NH_4Cl particle nucleation and growth at 253–296 K. Aerosol Sci. Tech. *2*, 321–339.

Hirschfelder, J. O., Curtiss, C. F., and Bird, R. B. (1954) *Molecular Theory of Gases and Liquids*, Wiley.

Homann, K. H., and Wagner, H. G. (1968) Chemistry of carbon formation in flames. Proc. Roy. Soc. A *307*, 141–152.

Jensen, D. E. (1974) Prediction of soot formation rates: a new approach. Proc. Roy. Soc. A *338*, 375–396.

Katz, J. L., and Donohue, M. D. (1982) Nucleation with simultaneous chemical reaction. J. Colloid Interface Sci. *85*, 267–277.

Lahaye, J., and Prado, G. (1974) Formation of carbon particles from a gas phase: Nucleation Phenomenon. Water, Air and Soil Pollution *3*, 473–481.

Liñán, A. (1974) The asymptotic structure of counter flow diffusion flames for large activation energies. Acta Astronautica *1*, 1007–1039.

Lothe, J., and Pound, G. M. (1962) Reconsideration of nucleation theory. J. Chem. Phys. *36*, 2080–2085.

Neville, M., and Sarofim, A. F. (1982) The stratified composition of inorganic submicron particles produced during coal combustion. *The Nineteenth Symposium (International) on Combustion*, 1441–1449, The Combustion Institute.

Springer, G. S. (1978) Homogeneous nucleation, *Adv. in Heat Transfer*, Vol. 14, 281–346, Academic Press.

Stein, S. E. (1978) On the high temperature chemical equilibria of polycyclic aromatic hydrocarbons. J. Phys. Chem. *82*, 566–571.

Tsuji, H., and Yamaoka, I. (1968) The structure of counterflow diffusion flames in the forward stagnation region of a porous cylinder. *The Twelfth Symposium (International) on Combustion*, 997–1005, The Combustion Institute.

Tsuji, H., and Yamaoka, I. (1970) Structure analysis of counterflow diffusion flames in the forward stagnation region of a porous cylinder. *The Thirteenth Symposium (International) on Combustion*, 723–731, The Combustion Institute.

Tsuji, H. (1982) Counterflow diffusion flames. Prog. Energy Combust. Sci. *8*, 93–119.

Vandsburger, U., Kennedy, I. M., and Glassman, I. (1984) Sooting counterflow diffusion flames with varying oxygen index, to appear in Combust. Sci. Tech.

Wakeshima, H. (1954) Time lag in self nucleation. J. Chem. Phys. *22*, 1614–1615.

Wegener, P. P., and Wu, B. J. C. (1977) Gasdynamics and homogeneous nucleation, in Nucleation Phenomena, 325–417, ed. A. C. Zettlemoyer, Elsevier.

Zettlemoyer, A. C. (1969) *Nucleation*, Dekker.

TABLE 1

Mass Fluxes (kg $m^{-3}s^{-1}$) Between Cluster Sizes

$D_1 = 10^8$, $\zeta = 10^{-4}$

Forward		*Reverse*
$\dot{\gamma}_{1\to2}$	$4{\cdot}74\times10^{-1}$	$4{\cdot}74\times10^{-1}$ $\dot{\gamma}_{1\leftarrow2}$
$\dot{\gamma}_{2\to3}$	$2{\cdot}52\times10^{-4}$	$2{\cdot}26\times10^{-4}$ $\dot{\gamma}_{2\leftarrow3}$
$\dot{\gamma}_{3\to4}$	$2{\cdot}47\times10^{-5}$	$1{\cdot}18\times10^{-5}$ $\dot{\gamma}_{3\leftarrow4}$
$\dot{\gamma}_{4\to5}$	$1{\cdot}20\times10^{-8}$	$1{\cdot}77\times10^{-9}$ $\dot{\gamma}_{4\leftarrow5}$
$\dot{\gamma}_{16\to17}$	$7{\cdot}86\times10^{-9}$	$3{\cdot}3\times10^{-31}$ $\dot{\gamma}_{16\leftarrow17}$
$\dot{\gamma}_{17\to18}$	$7{\cdot}86\times10^{-9}$	$3{\cdot}3\times10^{-31}$ $\dot{\gamma}_{17\leftarrow18}$
$\dot{\gamma}_{18\to19}$	$7{\cdot}84\times10^{-9}$	$3{\cdot}3\times10^{-31}$ $\dot{\gamma}_{18\leftarrow19}$

$D_1 = 10^6$, $\zeta = 10^{-4}$

$\dot{\gamma}_{1\to2}$	$4{\cdot}33\times10^{-1}$	$4{\cdot}24\times10^{-1}$ $\dot{\gamma}_{1\leftarrow2}$
$\dot{\gamma}_{2\to3}$	$2{\cdot}15\times10^{-4}$	$9{\cdot}58\times10^{-5}$ $\dot{\gamma}_{2\leftarrow3}$
$\dot{\gamma}_{3\to4}$	$1{\cdot}04\times10^{-5}$	$2{\cdot}51\times10^{-7}$ $\dot{\gamma}_{3\leftarrow4}$

TABLE 2

Mass Fluxes (kg $m^{-3}s^{-1}$) Between Cluster Sizes

$D_1 = 60$, $D_2 = 10^8$

Forward		*Reverse*
$\dot{\gamma}_{1\to2}$	$1{\cdot}32\times10^{-8}$	$1{\cdot}32\times10^{-8}$ $\dot{\gamma}_{1\leftarrow2}$
$\dot{\gamma}_{2\to3}$	$4{\cdot}77\times10^{-13}$	$4{\cdot}77\times10^{-13}$ $\dot{\gamma}_{2\leftarrow3}$
$\dot{\gamma}_{3\to4}$	$3{\cdot}55\times10^{-15}$	$3{\cdot}51\times10^{-15}$ $\dot{\gamma}_{3\leftarrow4}$
$\dot{\gamma}_{4\to5}$	$2{\cdot}43\times10^{-16}$	$1{\cdot}99\times10^{-16}$ $\dot{\gamma}_{4\leftarrow5}$

$D_1 = 0{\cdot}6$, $D_2 = 10^6$

$\dot{\gamma}_{1\to2}$	$1{\cdot}76\times10^{-12}$	$1{\cdot}76\times10^{-12}$ $\dot{\gamma}_{1\leftarrow2}$
$\dot{\gamma}_{2\to3}$	$7{\cdot}32\times10^{-19}$	$7{\cdot}32\times10^{-19}$ $\dot{\gamma}_{2\leftarrow3}$
$\dot{\gamma}_{3\to4}$	$6{\cdot}28\times10^{-23}$	$6{\cdot}28\times10^{-23}$ $\dot{\gamma}_{3\leftarrow4}$
$\dot{\gamma}_{4\to5}$	$5{\cdot}02\times10^{-26}$	$5{\cdot}01\times10^{-26}$ $\dot{\gamma}_{4\leftarrow5}$
$\dot{\gamma}_{5\to6}$	$2{\cdot}12\times10^{-28}$	$2{\cdot}08\times10^{-28}$ $\dot{\gamma}_{5\leftarrow6}$

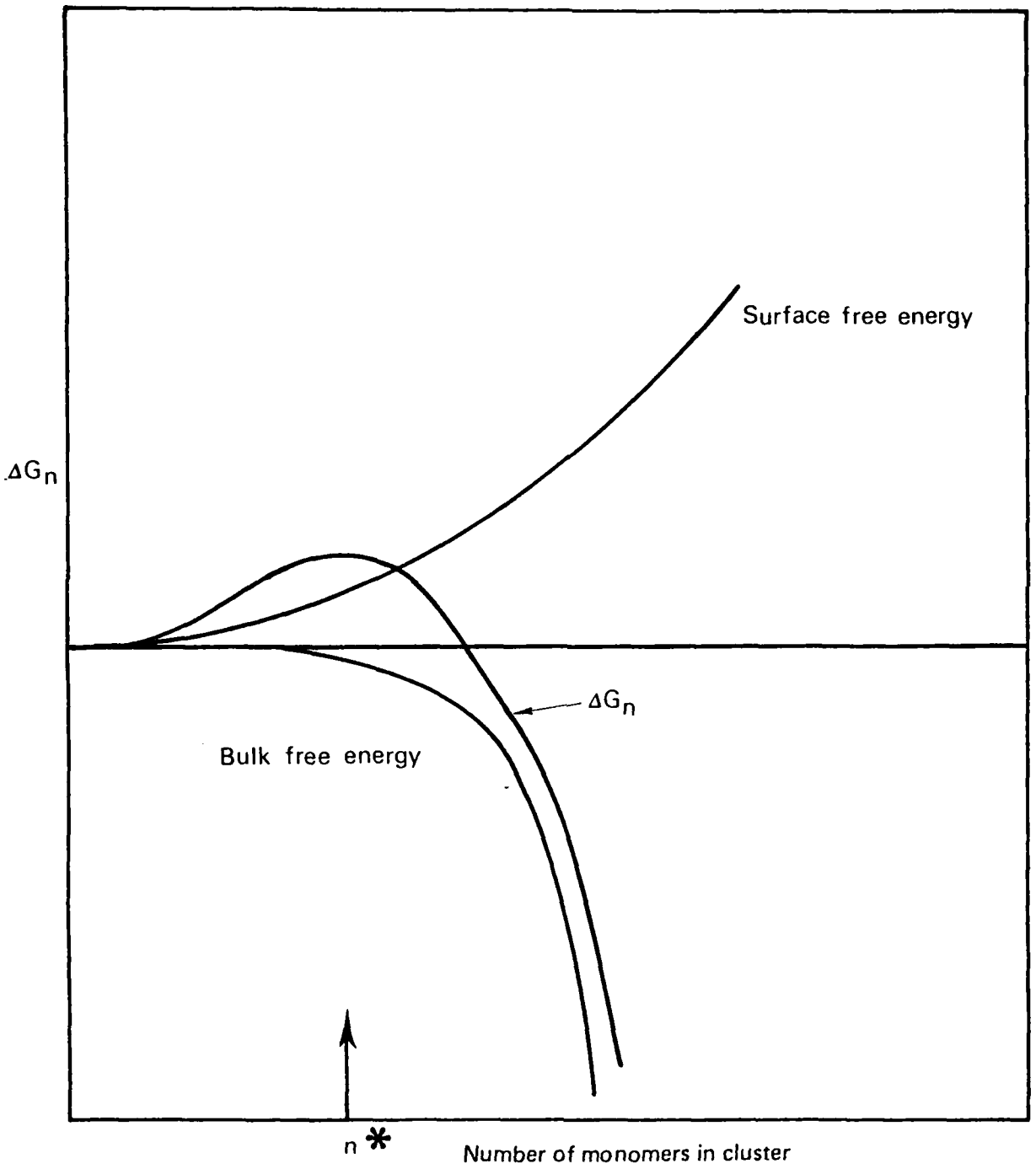

FIG. 1 VARIATION IN FREE ENERGY FUNCTIONS WITH CLUSTER SIZE.

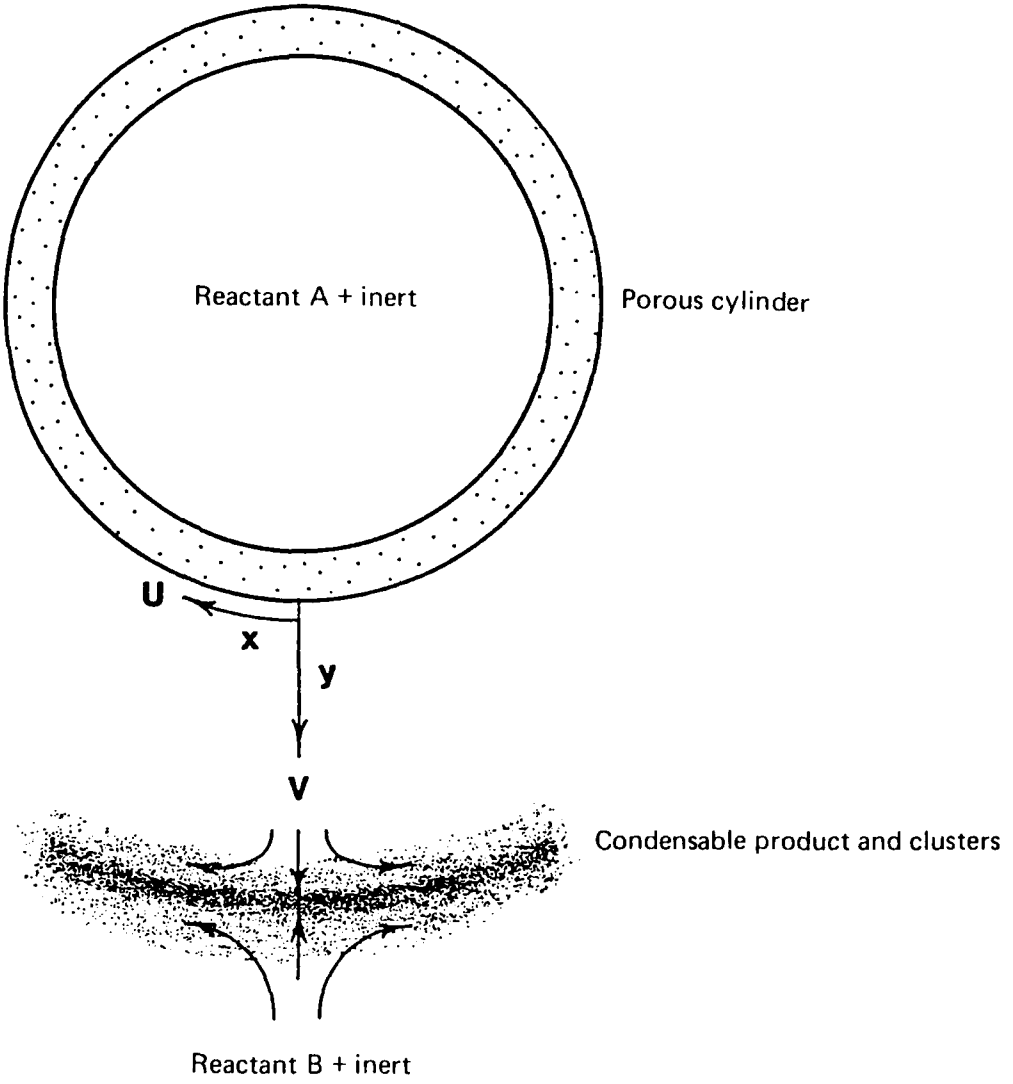

FIG. 2 STAGNATION POINT MIXING LAYER FLOW USED IN THE CALCULATIONS

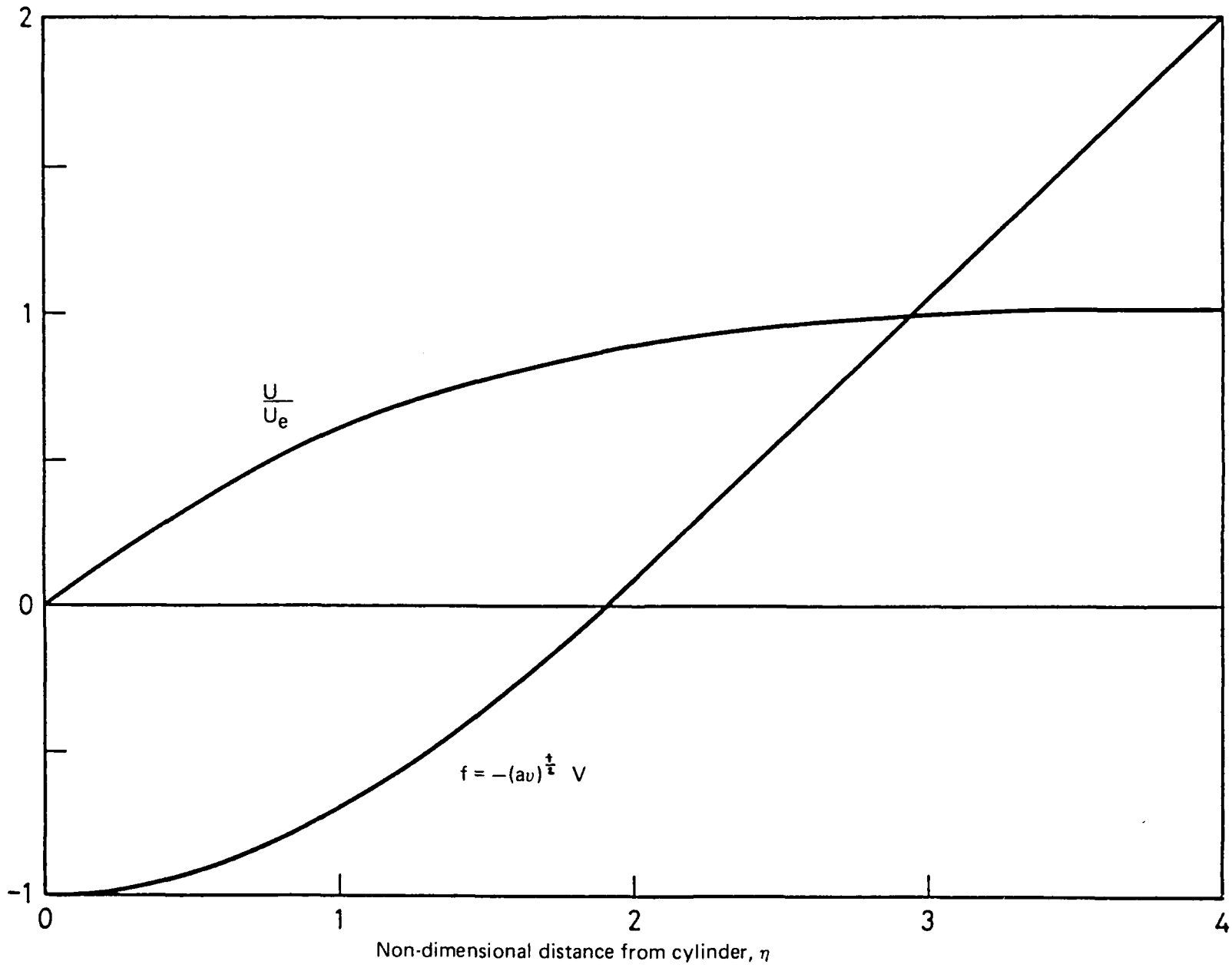

FIG. 3 MIXING LAYER VELOCITY PROFILES

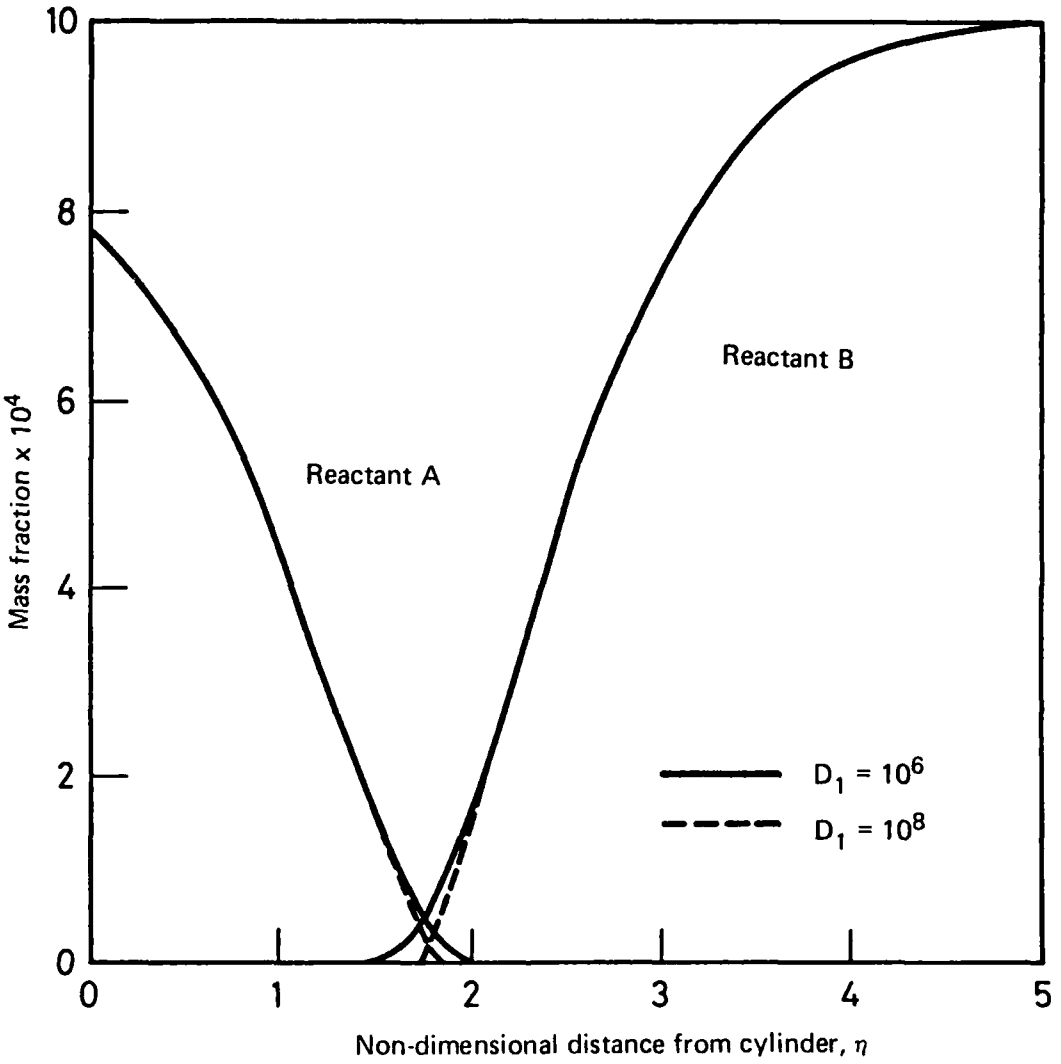

FIG. 4 MASS FRACTIONS OF REACTANTS A AND B WITH DISTANCE FROM CYLINDER

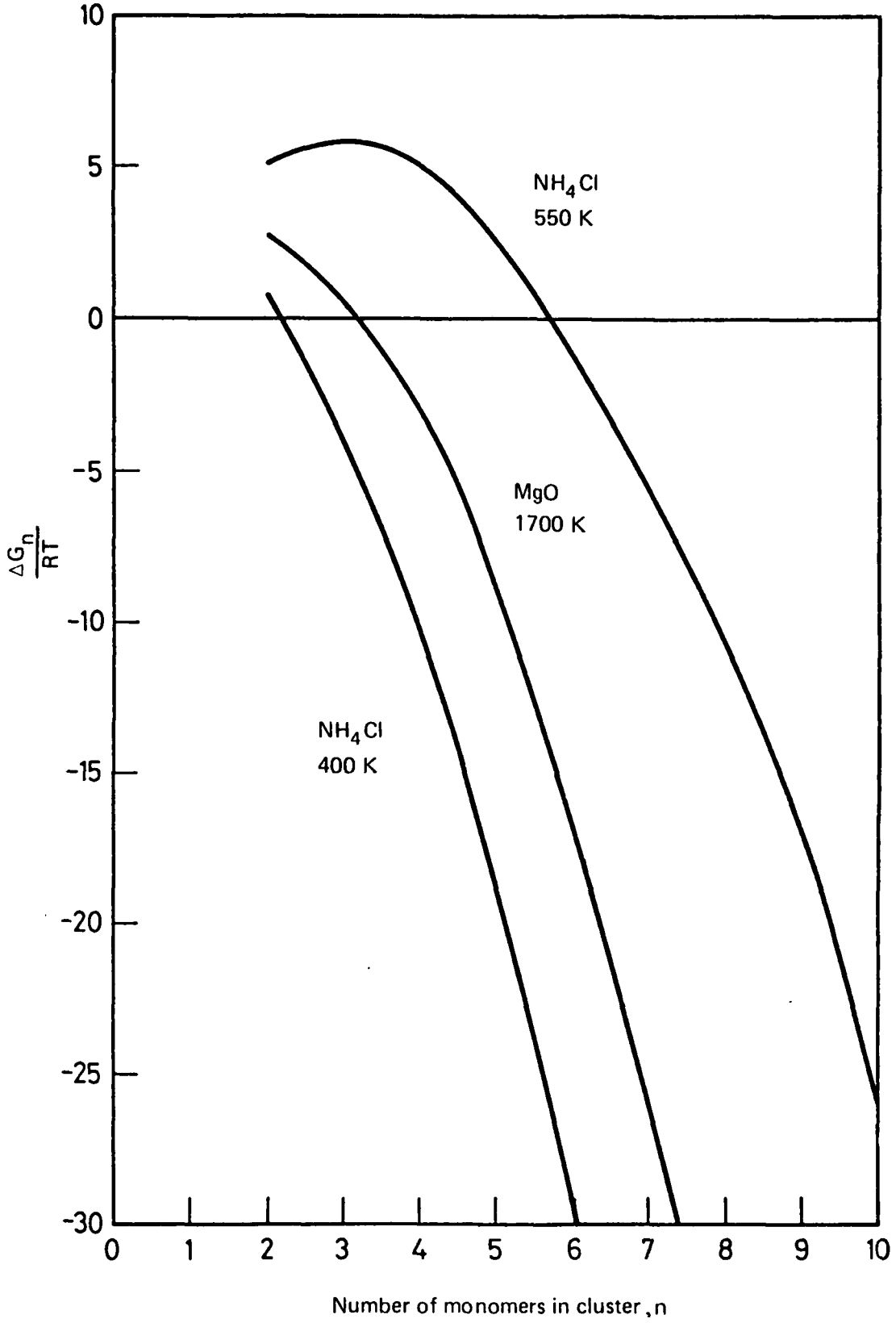

FIG. 5 ESTIMATED GIBBS FREE ENERGY FUNCTIONS FOR MONOMER ASSOCIATION

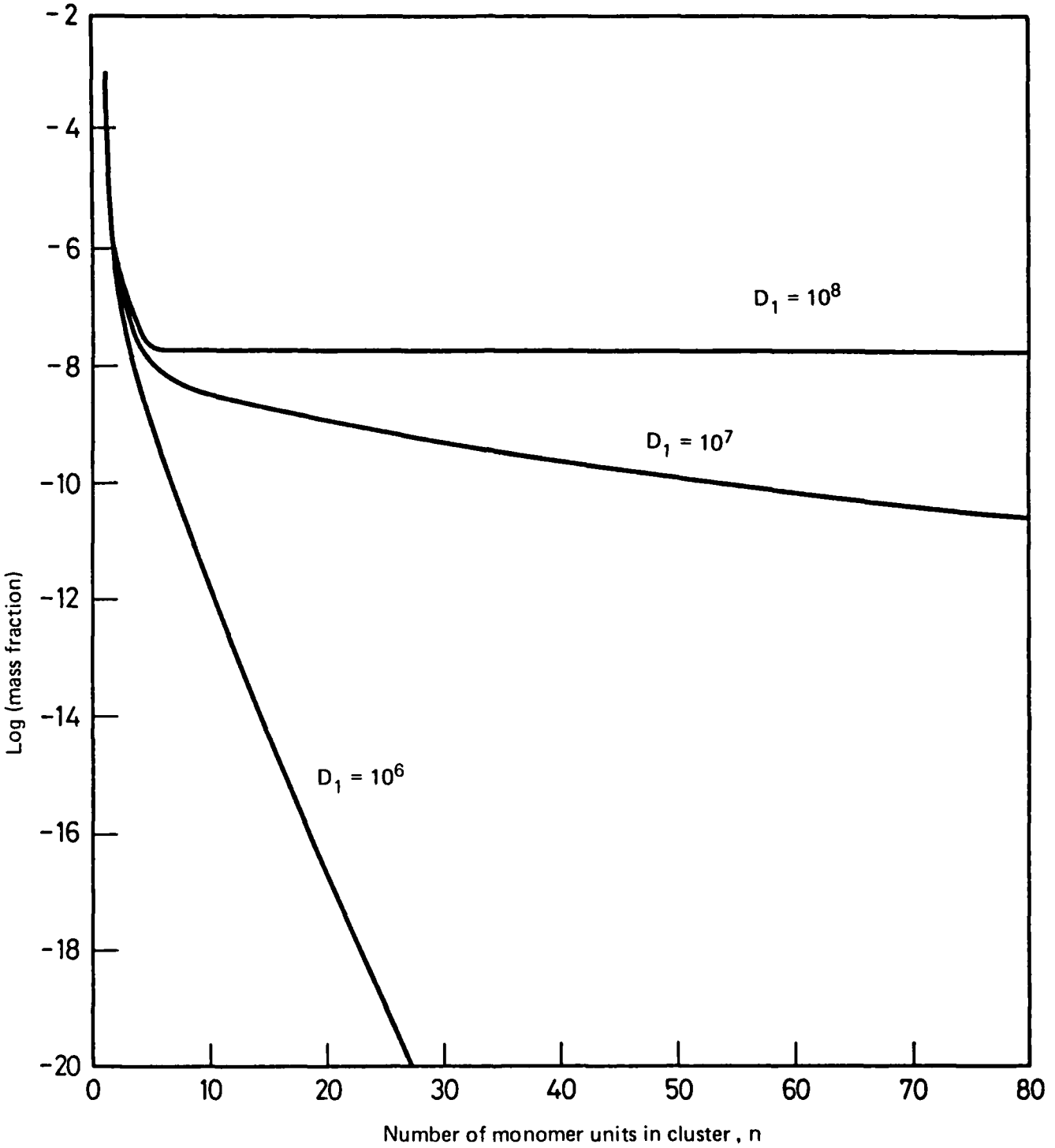

FIG. 6 CLUSTER MASS FRACTIONS AT STAGNATION POINT $\zeta = 10^{-4}$ AND ΔG_n FOR NH_4Cl AT 400 K

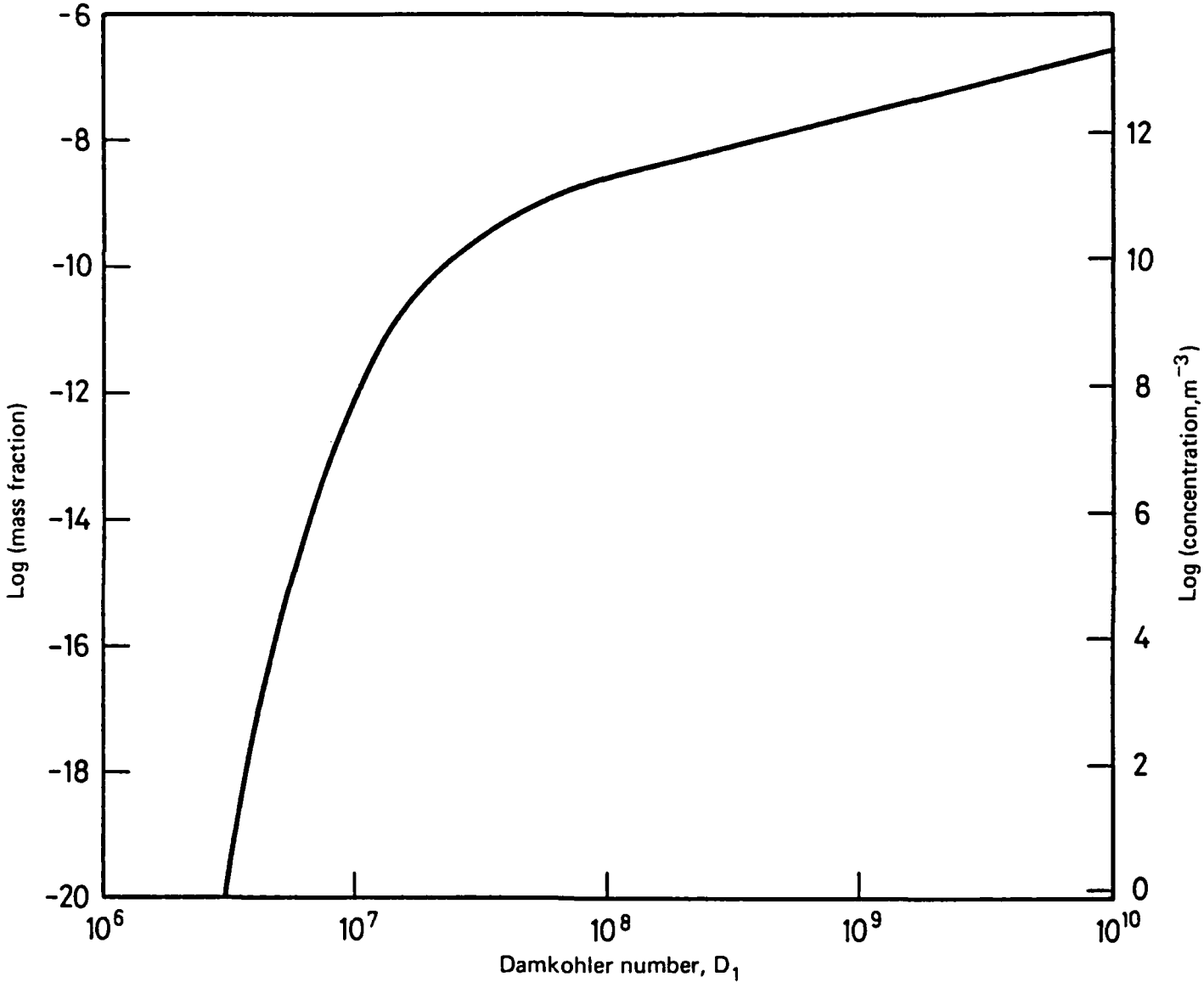

FIG. 7 MASS FRACTIONS AND CONCENTRATIONS AT STAGNATION POINT OF PARTICLES CONTAINING 200 MONOMER UNITS $\zeta = 10^{-4}$ AND ΔG_n FOR NH_4Cl AT 400 K

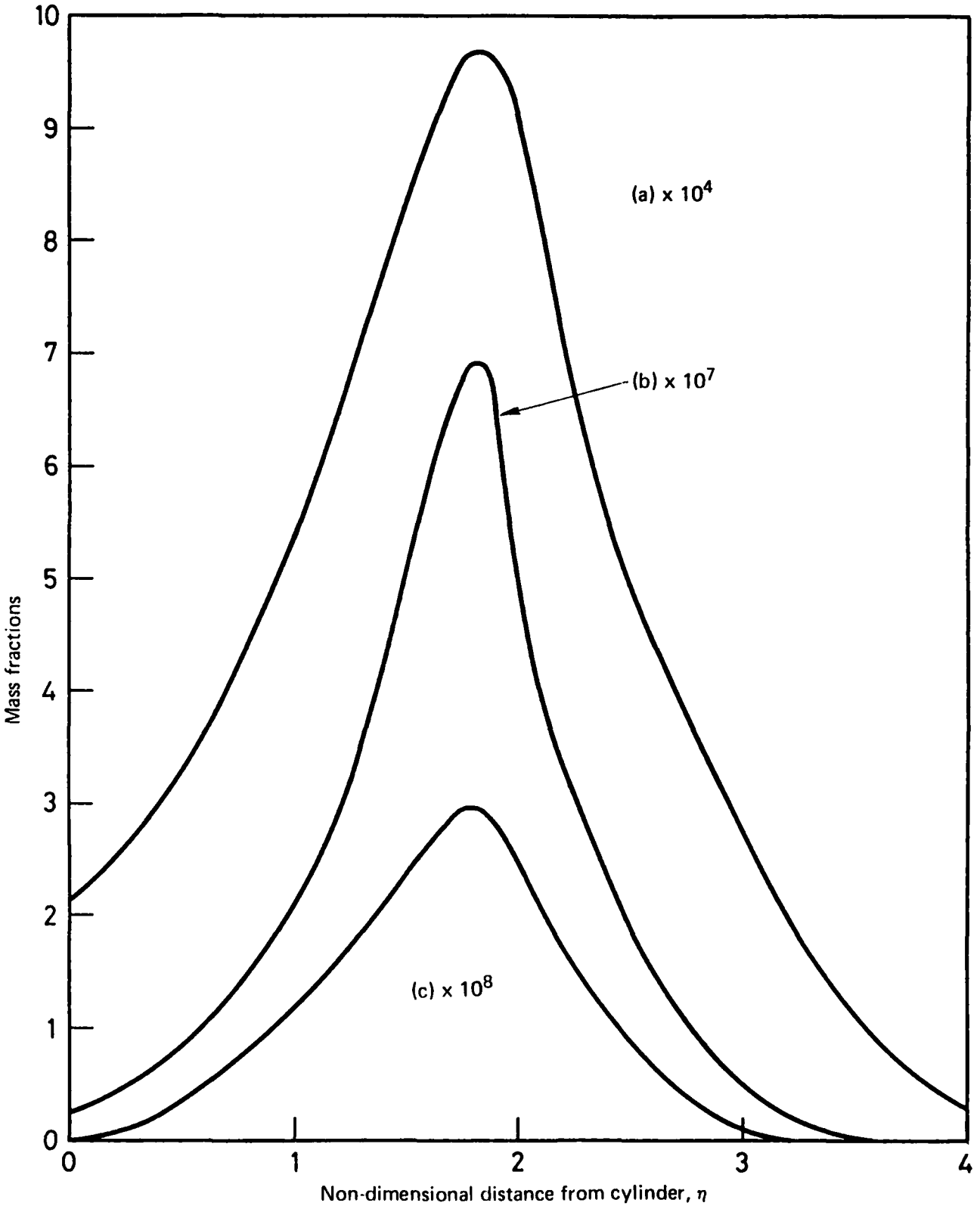

FIG. 8 DISTRIBUTION OF CLUSTERS THROUGH THE FLOW FOR CLUSTERS WITH
(a) 2 MONOMER UNITS
(b) 40 " "
(c) 80 " "
$\zeta = 10^{-4}$ AND ΔG_n FOR NH_4Cl AT 400 K

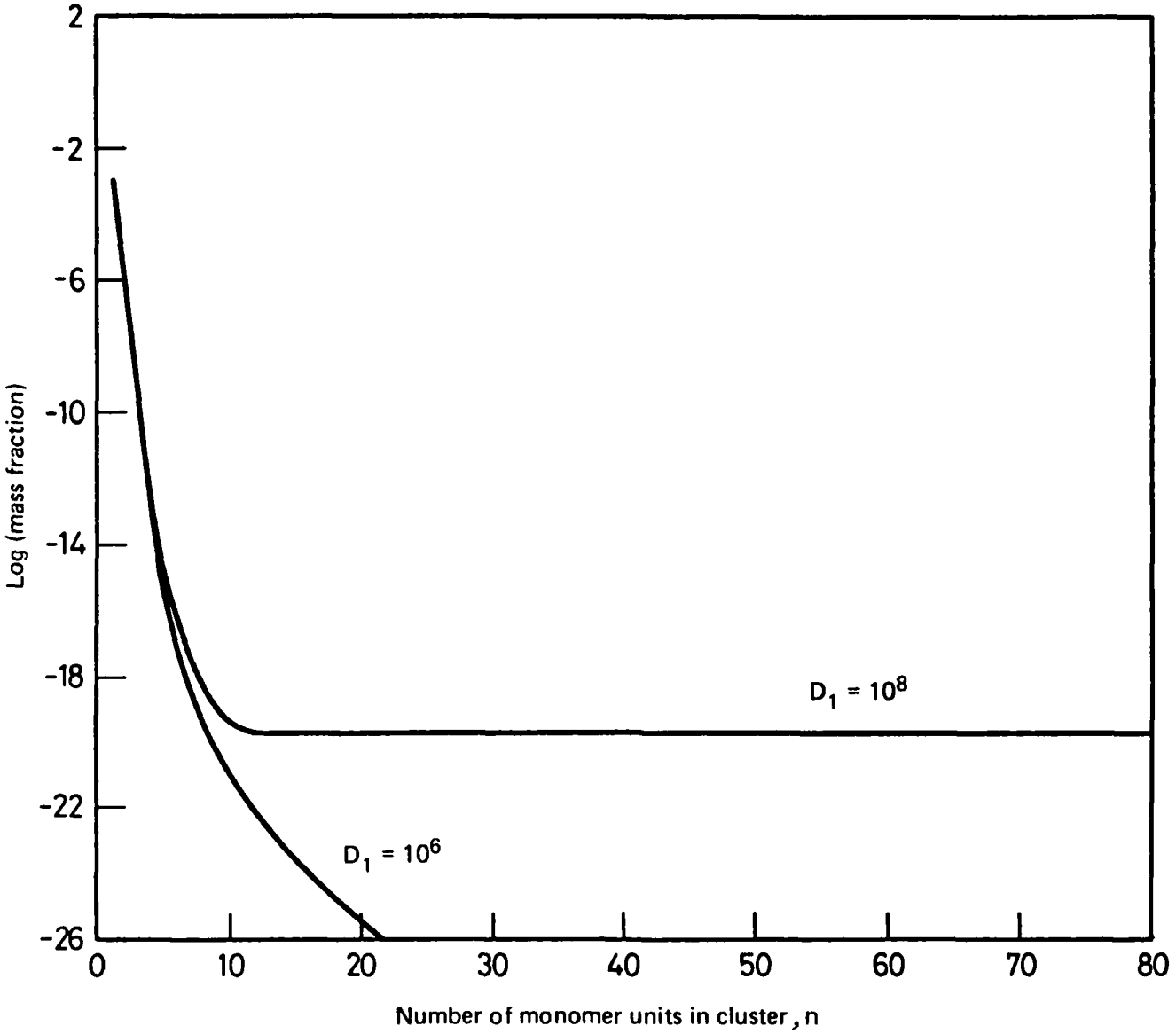

FIG. 9 CLUSTER MASS FRACTIONS AT STAGNATION POINT $\zeta = 10^{-4}$ AND ΔG_n FOR NH_4Cl AT 550 K

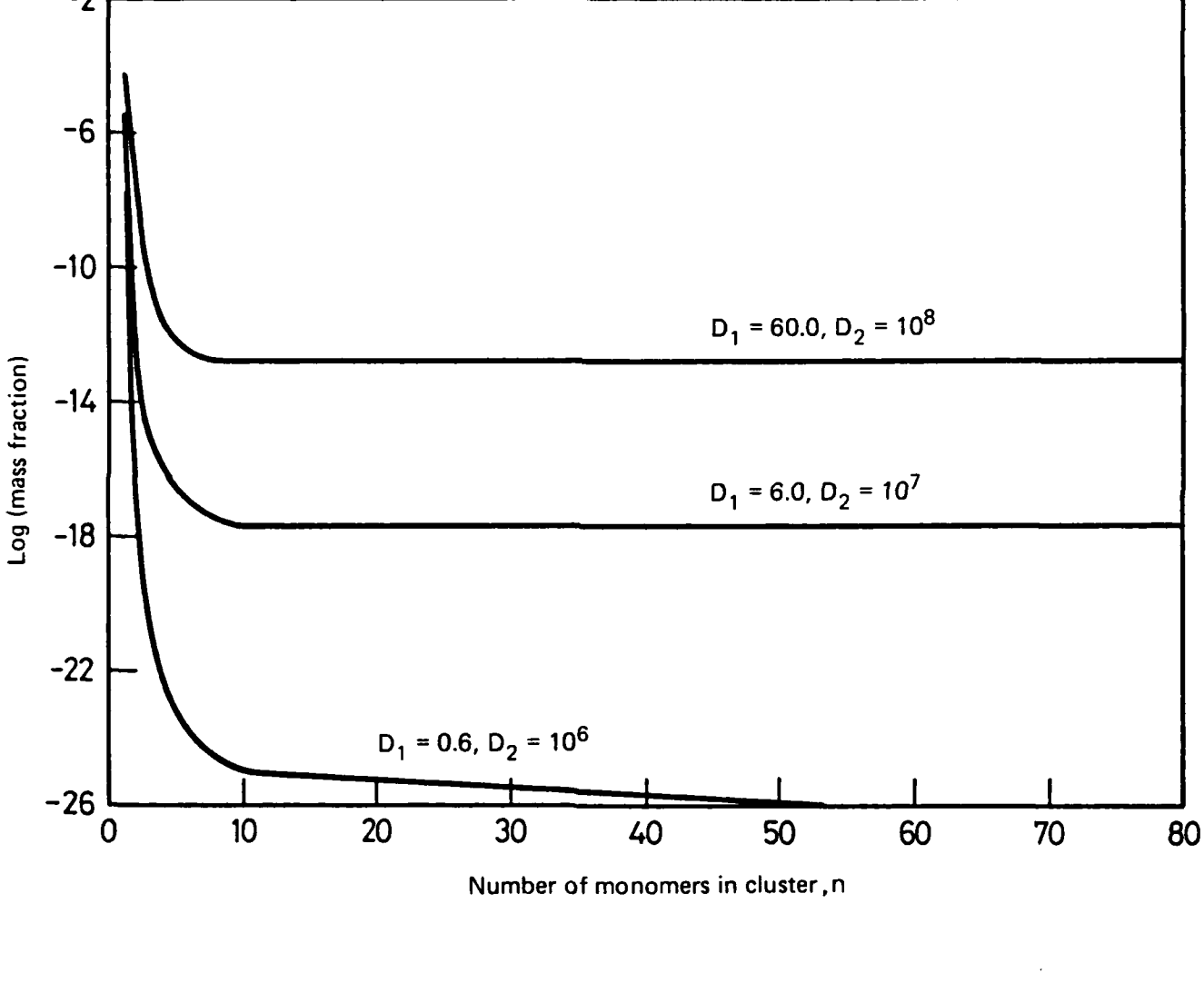

FIG. 10 CLUSTER MASS FRACTIONS AT STAGNATION POINT FOR SLOW MONOMER FORMATION RATES $\zeta = 1$ AND ΔG_n FOR NH_4Cl AT 400 K

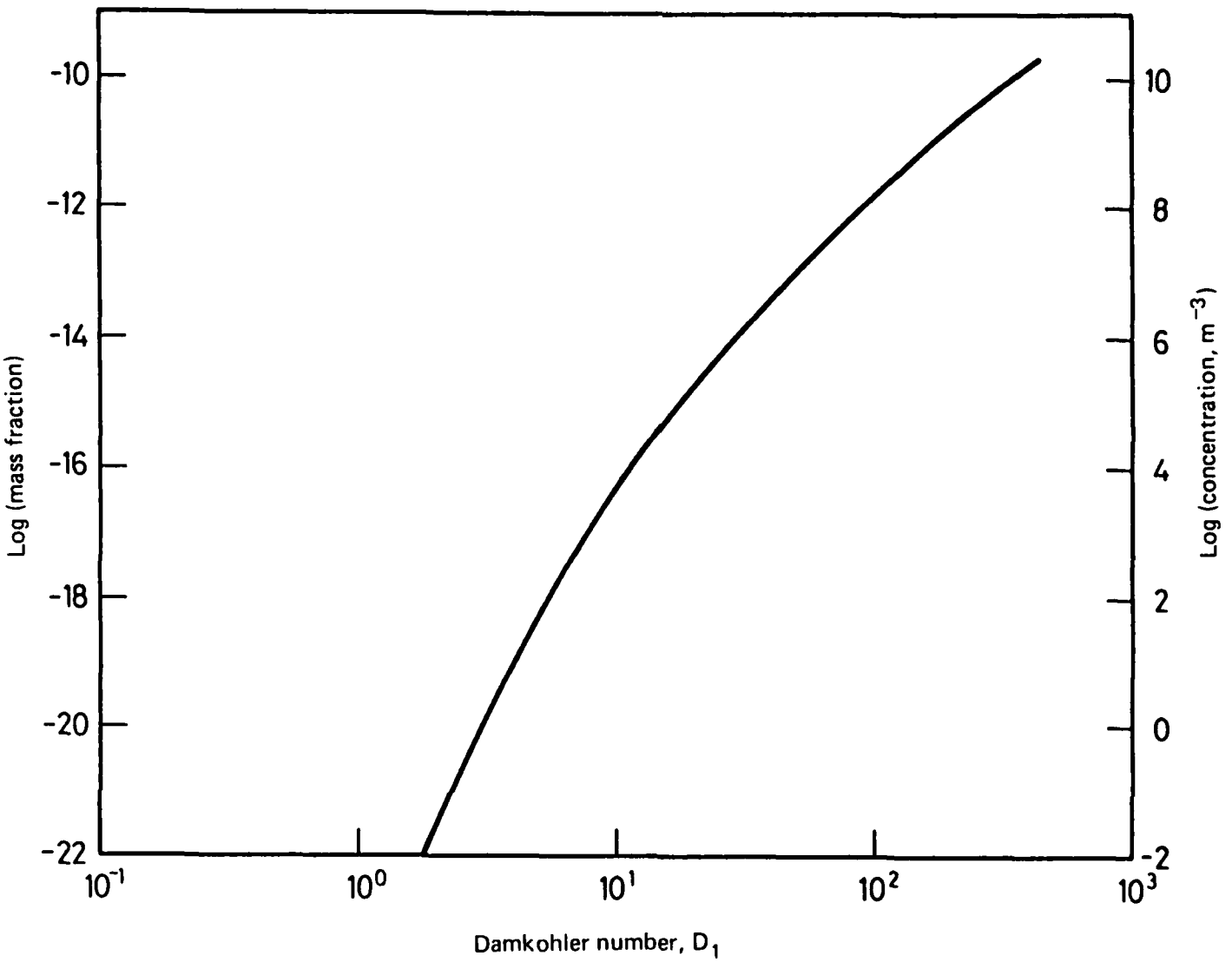

FIG. 11 MASS FRACTIONS AND CONCENTRATIONS AT STAGNATION POINT OF CLUSTERS CONTAINING 200 MONOMER UNITS $\zeta = 1$ AND ΔG_n FOR NH_4Cl AT 400 K

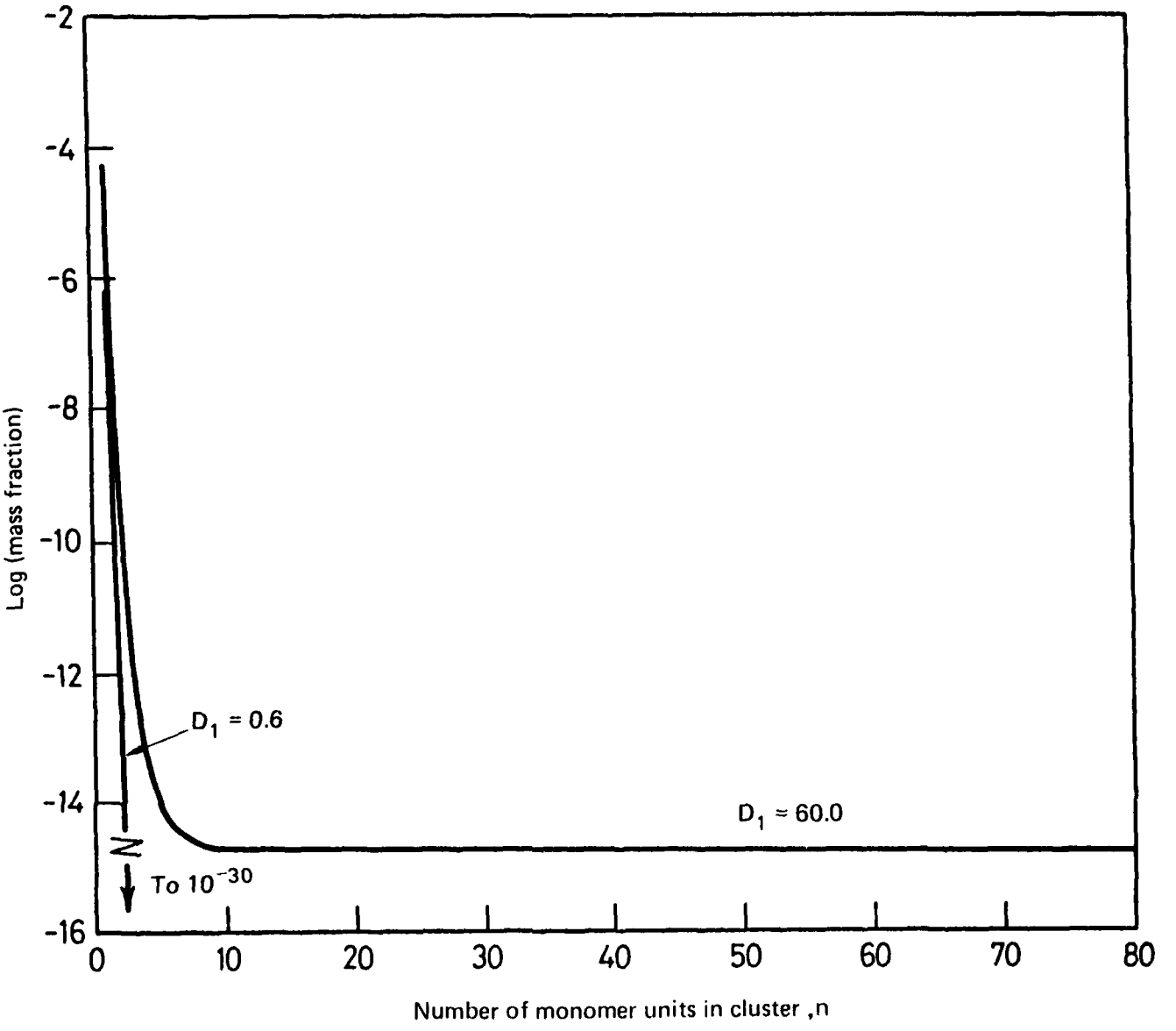

FIG. 12 CLUSTER MASS FRACTIONS AT STAGNATION POINT FOR SLOW MONOMER FORMATION RATES ζ = 1 AND ΔG_n FOR MgO AT 1700 K

DISTRIBUTION

AUSTRALIA

DEPARTMENT OF DEFENCE

Central Office

Chief Defence Scientist
Deputy Chief Defence Scientist
Superintendent, Science and Program Administration
Controller, External Relations, Projects and Analytical Studies
} (1 copy)

Defence Science Adviser (U.K.) (Doc. Data sheet only)
Counsellor, Defence Science (U.S.A.) (Doc. Data sheet only)
Defence Science Representative (Bangkok)
Defence Central Library
Document Exchange Centre, D.I.S.B. (18 copies)
Joint Intelligence Organisation
Librarian H Block, Victoria Barracks, Melbourne
Director General—Army Development (NSO) (4 copies)

Aeronautical Research Laboratories

Director
Library
Superintendent—Aero Propulsion
Divisional File—Aero Propulsion
Author: I. M. Kennedy
W. H. Schofield
L. W. Hillen
G. F. Pearce
F. W. Skidmore

Materials Research Laboratories

Director/Library

Defence Research Centre

Library

RAN Research Laboratory

Library

Navy Office

Navy Scientific Adviser

Army Office

Scientific Adviser—Army
Engineering Development Establishment, Library
Royal Military College Library
U.S. Army Research, Development and Standardisation Group

Air Force Office

Air Force Scientific Adviser
Aircraft Research and Development Unit
  Scientific Flight Group
  Library
Technical Division Library

Central Studies Establishment
Information Centre

STATUTORY AND STATE AUTHORITIES AND INDUSTRY

Australian Atomic Energy Commission, Director
CSIRO, Materials Science Division, Library
SEC of Vic., Herman Research Laboratory, Library

Universities and Colleges

Adelaide	Barr Smith Library
	Professor of Mechanical Engineering
Flinders	Library
Latrobe	Library
Melbourne	Engineering Library
Monash	Hargrave Library
Newcastle	Library
New England	Library
Sydney	Engineering Library
	Professor R. W. Bilger, Mechanical Engineering
	Professor R. I. Tanner, Mechanical Engineering
	Dr J. H. Kent, Mechanical Engineering
	Dr B. S. Haynes, Chemical Engineering
N.S.W.	Physical Sciences Library
	Professor R. A. A. Bryant, Mechanical Engineering
	Professor G. D. Sergeant, Fuel Technology
Queensland	Library
Tasmania	Engineering Library
Western Australia	Library
R.M.I.T.	Library

CANADA

International Civil Aviation Organization, Library
NRC
Aeronautical & Mechanical Engineering Library
Division of Mechanical Engineering, Director
Gas Dynamics Laboratory, Mr R. A. Tyler

CZECHOSLOVAKIA

Aeronautical Research and Test Institute (Prague), Head

FRANCE

ONERA, Library

GERMANY

Fachinformationszentrum: Energie, Physic, Mathematik GMBH

Universities and Colleges

Rheinisch-Westfalischen Technischen Hochschule	Institute fur Allgemeine Mechanik Professor N. Peters

INDIA

Defence Ministry, Aero Development Establishment, Library
Gas Turbine Research Establishment, Director
Hindustan Aeronautics Ltd., Library
National Aeronautical Laboratory, Information Centre

ISRAEL

Technion-Israel Institute of Technology
Professor J. Singer

ITALY

Professor Ing. Guiseppe Gabrielli
Instituto di Ricerche sulla Combustione, Dr A. D'Allessio

JAPAN

Institute of Space and Astronautical Science, Library

NETHERLANDS

National Aerospace Laboratory (NLR), Library

NEW ZEALAND

Defence Scientific Establishment, Library
Transport Ministry, Airworthiness Branch, Library
RNZAF, Vice Consul (Defence Liaison)

Universities

Canterbury	Library
	Professor D. Stevenson, Mechanical Engineering
	Mr J. Stott, Chemical Engineering

SWEDEN

Aeronautical Research Institute, Library
Swedish National Defense Research Institute (FOA)

SWITZERLAND

Armament Technology and Procurement Group
F+W (Swiss Federal Aircraft Factory)

UNITED KINGDOM

CAARC, Secretary
Royal Aircraft Establishment, Bedford, Library
Propellants, Explosives and Rocket Motor Establishment, Dr D. Jensen
National Gas Turbine Establishment, Director, Pyestock North
National Physical Laboratory, Library

National Engineering Laboratory, Library
British Library, Lending Division
CAARC Co-ordinator, Structures
Aircraft Research Association, Library
GEC Gas Turbines Ltd., Managing Director
Rolls-Royce Ltd., Aero Division Bristol, Library
British Aerospace, Hatfield-Chester Division, Library
British Hovercraft Corporation Ltd., Library
Short Brothers Ltd., Technical Library
Lucas CAV Limited, Dr D. Greeves

Universities and Colleges

Bristol	Engineering Library
Cambridge	Library, Engineering Department
	Whittle Library
Manchester	Library
Nottingham	Science Library
Southampton	Library
	Professor K. N. C. Bray, Aeronautics & Astronautics
Liverpool	Fluid Mechanics Division, Dr J. C. Gibbings
Strathclyde	Library
Cranfield Institute of Technology	Library
	Professor J. B. Moss, Mechanical Engineering
Imperial College	Chemical Eng. & Chemical Technol., Library
	Dr F. Lockwood, Mechanical Engineering

UNITED STATES OF AMERICA

NASA Scientific and Technical Information Facility
Applied Mechanics Reviews
Metals Information
The John Crerar Library
The Chemical Abstracts Service
Allis Chalmers Corporation, Library
Boeing Company, Mr J. C. McMillan
Kentex Research Library
United Technologies Corporation
  Library
  Research Center
    Dr J. J. Sangiovanni
    Dr L. Boedeker
Lockheed-California Company
Lockheed Missiles and Space Company
Lockheed Georgia
McDonnell Aircraft Company
  Dr J. M. Madson
  Library
Factory Mutual Research Corporation, Dr J. De Ris
General Motors Research Laboratories
  Dr S. J. Harris
  Dr G. W. Smith
National Bureau of Standards, Dr R. Santoro
Sandia National Laboratories, Dr W. Flower
  U.S. Rocket Propulsion Laboratory, Library

Universities and Colleges

Princeton	Mechanical & Aerospace Engineering Department
	Professor F. L. Dryer

	Professor I. Glassman
	Professor F. A. Williams
Massachusetts Institute of Technology	M.I.T. Libraries
	Professor A. Sarofim, Chemical Engineering
Stanford	Professor C. T. Bowman, Dept. of Mechanical Engineering
California	Professor C. K. Law, Department of Mechanical Engineering
Dayton	Dr L. Krishnamurthy
Southern California	Dr J. C. Lasheras, Department of Mechanical Engineering
Cornell	Professor S. H. Bauer
Johns Hopkins	Professor J. L. Katz
Yale	Professor D. E. Rosner

SPARES (15 copies)

TOTAL (174 copies)

Department of Defence

DOCUMENT CONTROL DATA

1. a. AR No.	1. b. Establishment No.	2. Document Date	3. Task No.
AR-003-972	ARL-AERO-PROP-R-165	November 1984	DST 82/045

4. Title	5. Security	6. No. Pages
FLOW FIELD EFFECTS ON NUCLEATION IN A REACTING MIXING LAYER	a. document: Unclassified b. title: U. c. abstract: U.	22 7. No. Refs: 37

8. Author(s)	9. Downgrading Instructions
I. M. Kennedy	—

10. Corporate Author and Address	11. Authority (*as appropriate*)
Aeronautical Research Laboratories P.O. Box 4331, Melbourne, Vic., 3001	a. Sponsor c. Downgrading b. Security d. Approval

12. Secondary Distribution (*of this document*)

Approved for public release

Overseas enquirers outside stated limitations should be referred through ASDIS, Defence Information Services Branch, Department of Defence, Campbell Park, CANBERRA, ACT, 2601.

13. a. This document may be ANNOUNCED in catalogues and awareness services available to . . .

No limitations

13. b. Citation for other purposes (*i.e. casual announcement*) may be (select) unrestricted (*or*) as for 13 a.

14. Descriptors	15. COSATI Group
Aerosols	07040
Nucleation	20040
Condensing	21020
Combustion products	
Rocket exhaust	
Soot	

16. Abstract

Chemical nucleation has been studied numerically in a stagnation point mixing layer in which reactants in two counter-flowing streams form a condensable monomer. The response of the subsequent nucleation kinetics to the velocity gradient in the flow is described in terms of a Damkohler number. Two limiting cases have been established. Firstly, if the Damkohler number for monomer production is small, i.e. the rate of monomer production is slow, then the nucleation of particles can be strongly affected by the flow field in a manner which is equivalent to the effect of supersaturation in a uniform vapour. Secondly, if the Damkohler numbers for cluster growth are small (due to a small accommodation factor for monomer-cluster interactions), the concentrations of clusters do not achieve equilibrium levels. This can result in the suppression of particle formation over a critical range of Damkohler numbers. In this case the behaviour of the nucleation kinetics is analogous to the transient phase of nucleation in a uniform vapour.

This page is to be used to record information which is required by the Establishment for its own use but which will not be added to the DISTIS data base unless specifically requested.

16. Abstract (*Contd*)

17. Imprint

Aeronautical Research Laboratories, Melbourne

18. Document Series and Number	19. Cost Code	20. Type of Report and Period Covered
Aero Propulsion Report 165	437410	

21. Computer Programs Used

22. Establishment File Ref(s)

END

FILMED

11-85

DTIC